Journal of Physiology (1993), **464**, *pp.* 501–528
With 10 figures
Printed in Great Britain

Ca^{2+}-DEPENDENT INACTIVATION OF Ca^{2+} CURRENT IN *APLYSIA* NEURONS: KINETIC STUDIES USING PHOTOLABILE Ca^{2+} CHELATORS

BY MARTIN W. FRYER* AND ROBERT S. ZUCKER

From the Department of Molecular and Cell Biology, University of California, Berkeley, CA 94720, USA

(*Received 23 March 1992*)

SUMMARY

1. The kinetics and sensitivity of the Ca^{2+}-dependent inactivation of calcium current (I_{Ca}) were examined in intact cell bodies from the abdominal ganglion of *Aplysia californica* under two-electrode voltage clamp.

2. Rapid changes in the level of intracellular free calcium ($[Ca^{2+}]_i$) were generated at the cell surface by photolytic release of Ca^{2+} (nitr-5 and dimethoxy nitrophen) or Ca^{2+} buffer (diazo-4).

3. Diazo-4 increased I_{Ca} by 10–15 % and slowed the rate of I_{Ca} decay when photolysed before a test pulse or between a prepulse and a test pulse. The predominant effect of further light flashes was to increase the amount of non-inactivating current (I_∞) remaining at the end of long (> 1 s) depolarizing pulses.

4. A rapid increase in $[Ca^{2+}]_i$ buffering during I_{Ca} inactivation did not cause a rapid recovery of current but merely reduced the rate and extent of subsequent inactivation. This effect was not seen when Ba^{2+} was the charge carrier.

5. Photolytic release of Ca^{2+} from nitr-5 produced estimated Ca^{2+} jumps of 3–4 μM at the front surface of the cell but failed to augment inactivation either before or during I_{Ca}. In contrast, photolysis of DM-nitrophen 10–90 ms before the test pulse decreased peak I_{Ca} by about 30 %. A flash given during I_{Ca} rapidly blocked 41 $\pm$ 3 % of peak current with a time constant of 3–4 ms at 17 °C. Similar results were seen with the barium current (I_{Ba}).

6. Microinjection of the potent phosphatase inhibitor microcystin-LR (5 μM) had variable effects on I_{Ca} inactivation and augmented the cyclic AMP-induced depression of the delayed rectifier ($I_{K(V)}$) by forskolin (100 μM) and 3-isobutyl-1-methylxanthine (IBMX; 200 μM).

7. Full recovery from inactivation measured in two-pulse experiments took at least 20 s. This slow recovery process was unaffected by increases in intracellular cyclic AMP elicited by direct injection or by bath application of forskolin and IBMX. It was also unaffected by decreases in cyclic AMP induced by injecting 2′,5′-dideoxyadenosine (1 mM) or bath application of the Rp isomer of cyclic adenosine 3′, 5′-monophosphothioate (Rp-cAMPS; 200 μM).

* To whom reprint requests should be sent at the Department of Zoology, La Trobe University, Bundoora, 3083, Australia.

MS 1227

8. A 'shell' model relating submembrane Ca^{2+} to inactivation was inconsistent with the experimental results since it greatly overestimated the effects of diazo-4 and predicted significant inactivation by nitr-5 photolysis.

9. A model linearly relating $[Ca^{2+}]_i$ in a single Ca^{2+} channel 'domain' to inactivation more closely matched the experimental results with diazo-4 and DM-nitrophen if Ca^{2+} binds to an inactivation site about 25 nm from the channel mouth with relatively low affinity (i.e. with a K_D of at least tens of micromolar). Since such high $[Ca^{2+}]_i$ levels only occur near a channel after opening, we suggest that inactivation normally only proceeds from the open-channel state.

10. A simple kinetic scheme based on the rapid inactivation of open calcium channels by Ca^{2+} is presented which successfully predicts the chief characteristics of macroscopic inactivation.

INTRODUCTION

Inactivation of the macroscopic neuronal Ca^{2+} current (I_{Ca}) in *Aplysia californica* is predominantly mediated by an increase in the intracellular free Ca^{2+} concentration ($[Ca^{2+}]_i$) and displays little voltage dependence (Eckert & Tillotson, 1981; Eckert & Ewald, 1983; Eckert & Chad, 1984). Inactivation is experimentally observed as either the decline of I_{Ca} during a long depolarizing pulse or as the loss of peak current in a test pulse following a prepulse. This phenomenon is seen to varying degrees in many other invertebrate and vertebrate neurons and has been extensively reviewed (Eckert & Chad, 1984; Chad, 1989).

Despite the large body of evidence supporting this general mechanism there is little specific information regarding the location, sensitivity and kinetics of the interaction between $[Ca^{2+}]_i$ and the inactivation site. The Ca^{2+} sensitivity of the inactivation site in intact neurons has previously been inferred from experiments in which resting $[Ca^{2+}]_i$ has been manipulated by the intracellular injection of Ca^{2+} or Ca^{2+}–buffer mixtures (Eckert & Tillotson, 1981; Plant, Standen & Ward, 1983; Chad, Eckert & Ewald, 1984; Gutnick, Lux, Swandulla & Zucker, 1989). While these studies provide information about the effects of changes in steady-state $[Ca^{2+}]_i$ on inactivation, they do little to mimic the spatial and temporal changes in $[Ca^{2+}]_i$ that are believed to occur in the Ca^{2+} 'domain' surrounding each individual Ca^{2+} channel during activation (Chad & Eckert, 1984; Simon & Llinás, 1985; Zucker & Fogelson, 1986; Sherman, Keizer & Rinzel, 1990).

Recently, two photolabile calcium chelators (nitr-5 : Adams, Kao, Minta, Grynkiewicz & Tsien, 1988; dimethoxy (DM) nitrophen : Kaplan & Ellis-Davies, 1988) have been developed that can elicit rapid (i.e. < 1 ms) increases in Ca^{2+} after photolysis by ultraviolet (UV) light. DM-nitrophen has already been successfully used to characterize the onset kinetics of Ca^{2+}-dependent inactivation of I_{Ca} currents in perfused chick dorsal root ganglion cells (Morad, Davies, Kaplan & Lux, 1988) and *Lymnaea* snail neurons (Johnson & Byerly, 1991). A possible problem in these whole-cell perfusion experiments is the wash-out of cytoplasmic factors (such as kinases and phosphatases) that might regulate Ca^{2+}-dependent inactivation (Chad & Eckert, 1986; Armstrong & Eckert, 1987; Armstrong, 1989). This explains the importance of studying inactivation in intact neurons.

In this paper, the onset kinetics of Ca^{2+}-dependent inactivation are investigated in intact *Aplysia* neurons using DM-nitrophen. This approach is complemented by using the novel photolabile BAPTA (1,2-bis(*O*-aminophenoxy)ethane-*N*,*N*,*N*′,*N*′,-tetraacetic acid) derivative diazo-4 (Adams, Kao & Tsien, 1989) to produce rapid drops in $[Ca^{2+}]_i$ before, during and after the development of Ca^{2+}-dependent inactivation. Finally, Ca^{2+}-dependent inactivation is studied in metabolically altered neurons to address its possible regulation by phosphorylation and dephosphorylation.

Preliminary accounts of some of these experiments have been previously published in abstract form (Fryer & Zucker, 1990, 1991).

METHODS

Experiments were performed on single identified cells in abdominal ganglia dissected from *Aplysia californica*. Details of the ganglion removal, desheathing, axotomy and solution changes have been previously described (Kramer & Zucker, 1985; Landò & Zucker, 1989). Most experiments were done on axotomized left upper quadrant neurons, particularly L3 and L6 which have been shown to possess a Ca^{2+}-activated K^+ conductance ($I_{K(Ca)}$) that is largely abolished by extracellular tetraethylammonium (TEA^+) ions (Deitmer & Eckert, 1985). Other, non-axotomized cells used that displayed robust Ca^{2+} currents were R15 and L8. Cell body diameters ranged from 200 to 400 μm. All results in this paper are from cells that had stable resting potentials more negative than −40 mV or displayed bursting in normal artificial sea water. Experiments were carried out at a temperature of 17 ± 0·2 °C (maintained with a Peltier effect cooler) unless otherwise noted.

Voltage clamp

Details of the two-electrode voltage clamp technique employed have been previously described (Smith & Zucker, 1980; Kramer & Zucker, 1985). In all I_{Ca} experiments, the voltage and current electrodes were filled with 3 M CsCl and had resistances of 1–5 MΩ. The calculated series resistance error for the magnitude of the currents in this paper (< 0·5 μA) was less than 1 mV and was not compensated. All currents (unless otherwise noted) have had linear leak and capacitive current transients subtracted using the 'P/2' or 'P/3' hyperpolarizing step procedure (Chad & Eckert, 1986). In some cases, the 'difference' I_{Ca} is shown, i.e. the difference between the raw I_{Ca} and the residual current after block by 15 min perfusion with 10 mM Co^{2+}.

Stimulus protocols and data aquisition were controlled by an AXOLAB-1 interface using either AXESS (version 1.0) or pClamp (version 5.0) software (Axon Instruments, Burlingame, CA, USA). In most experiments the acquisition speed was 2–5 kHz. All analysis and post-processing of data was done using pClamp (version 5.0). The variability among measurements is expressed as the mean ± standard error of the mean.

Solutions

Extracellular. The normal artificial sea water (NASW) contained (mM): NaCl, 490; KCl, 15; $CaCl_2$, 10; $MgCl_2$, 50; Na-Hepes, 10. For I_{Ca} studies TEA^+ was substituted for Na^+ and K-Hepes substituted for Na-Hepes with the KCl decreased to maintain the same total K^+. For Ba^{2+} current (I_{Ba}) studies, Ba^{2+} was substituted for Ca^{2+}. At the end of most experiments I_{Ca} and I_{Ba} were blocked with a similar solution that contained Co^{2+} in place of the Ca^{2+} or Ba^{2+}. All solutions had a final pH of 7·5 and contained tetrodotoxin (TTX; 30 μM) and 4-aminopyridine (4-AP; 4 mM). In experiments on the delayed rectifier K^+ current ($I_{K(V)}$) tetramethylammonium (TMA^+) replaced TEA^+, Co^{2+} replaced Ca^{2+} and 4-AP was omitted.

Forskolin and 3-isobutyl-1-methylxanthine (IBMX) (Sigma Chemical Co., St Louis, MO, USA) and the Rp isomer of cyclic adenosine 3′, 5′-monophoshothioate (Rp-cAMPS) (BioLog Life Science Inst., Bremen, Germany) were diluted in the appropriate saline to the desired concentration and applied directly to the bath. The stock solution of forskolin was 25 mM dissolved in ethanol. IBMX and Rp-cAMPS solutions were freshly prepared for each experiment.

Diazo-4. Samples of diazo-4 were generously donated by Drs R. Y. Tsien and S. R. Adams (Department of Pharmacology, University of California, San Diego, CA, USA). The chemical and kinetic properties of the diazo series of photolabile chelators have been previously described (Adams *et al.* 1989). Stock solutions contained 50–100 mM diazo-4 and 100–200 mM K-Hepes, pH 7·5. The final solution used for pressure microinjection contained 30–60 mM diazo-4, 1·5 M CsCl (for further suppression of contaminating K^+ currents) and 3–6 mM arsenazo III. CsCl was omitted in experiments designed to test the effects of intracellular diazo-4 alone (Fig. 1*A* and *B*). In some experiments, the absorbance of the neuron was monitored at the isosbestic point of arsenazo (577 nm) during injection (Smith & Zucker, 1980; Landò & Zucker, 1989). This allowed us to estimate the final concentrations of arsenazo and diazo-4 in the cell.

We used diazo-4 instead of diazo-2 because it has two photolysable diazoacetyl groups instead of one and thus undergoes a much larger affinity change for Ca^{2+} than diazo-2 upon photolysis (1600-fold *versus* 40-fold). The higher Ca^{2+} affinity of unphotolysed diazo-2 (dissociation constant, K_D, ≈ 4 μM, 0·25 M ionic strength) compared to diazo-4 ($K_D \approx 180$ μM, 0·25 M ionic strength) would result in a stronger competition with the native cell buffers and thus greatly attenuate Ca^{2+}-dependent processes prior to photolysis. In fact, even unphotolysed diazo-4 altered the intrinsic Ca^{2+} buffering when injected into neurons at millimolar concentrations (Fig. 1).

DM-nitrophen. DM-nitrophen was a gift from Drs J. Kaplan and G. Ellis-Davies (Department of Physiology, University of Pennsylvania, Philadelphia, PA, USA). In a few later experiments we used commercially available DM-nitrophen (Calbiochem) and saw no qualitative differences. Stock solutions of 60 mM DM-nitrophen were 30–60 % loaded with Ca^{2+} (i.e. 18–36 mM). Arsenazo (2 mM) and CsCl (1·5 M) were added to these solutions for microinjection. Peak I_{Ca} was typically reduced by 10–25 % after pressure injection of DM-nitrophen to a final intracellular concentration of 5–7 mM.

Other. Microcystin-LR (Sigma) and 2′,5′-dideoxyadenosine (DDA) (Pharmacia LKB Biotechnology, Uppsala, Sweden) were dissolved in a 200 mM KCl–10 mM Hepes buffer (pH 7·5) and pressure injected to give a final cytoplasmic concentration of 5 μM and 1–2 mM respectively. The stock solution of microcystin-LR was 5 mM dissolved in dimethyl sulphoxide (DMSO). Cyclic AMP was dissolved in distilled water to 0·1 M and either pressure injected or ionophoresed at −100 to −200 nA for 30–60 s.

Flash photolysis and spectrophotometry

The equipment and procedures used for flash photolysis and *in vitro* spectrophotometry have been extensively documented elsewhere (Tsien & Zucker, 1986; Landò & Zucker, 1989; Delaney & Zucker, 1990). A 200 J electrical discharge (corresponding to about 190 mJ cm^{-2} of light energy in 0·5 ms) photolysed 30 % of 50 % Ca^{2+}-loaded DM-nitrophen and 30 % of 3 % Ca^{2+}-loaded diazo-4 in microcuvettes. In cells, this amount of photolysis occurs near the front surface where the light intensity is greatest. Volume-average changes in the amount of photolysed compound depend on the cell volume as well as the UV absorbance properties of both the compound and the cell. After the flash the concentration of photolysis products at the front surface decreases as diffusion and subsequent equilibration occur throughout the cell. Following the 2 min post-flash equilibration period used in some of the experiments we estimate that 5 % of the volume-average diazo-4 is photolysed in a 300 μm diameter cell (see Appendix). In some experiments, a steady, low intensity collimated light beam was used for photolysis. A 2 s exposure to this light source photolysed the same amount of photolabile chelator as a 200 J flash.

Calculation of percentage photolysis

DM-nitrophen. To estimate the percentage photolysis of DM-nitrophen, microcuvettes (100 μm pathlength) were filled with a mixture of fura-2 (500 μM), DM-nitrophen (2 mM, 50 % Ca^{2+} loaded) dissolved in 100 mM KCl and 10 mM potassium 3-(*N*-morpholino)propanesulphonate (K-Mops), pH 7·0. After each photolysis a ratiometric image (350 and 385 nm excitation, 510 nm emission) was taken using a × 10 lens and Nikon (Garden City, NY, USA) Optiphot microscope equipped with a Dage (Michigan City, IN, USA) silicon-intensified target camera (Model 66). Comparison of the imaged fluorescence ratios with those from fura-2 calibrated in the presence of DM-nitrophen (Zucker, 1992) allowed the calculation of steady-state values of Ca^{2+} after each flash. These values were compared with those generated by a computer model similar to that described earlier

(Delaney & Zucker, 1990). This model solves the equilibrium reactions of unphotolysed DM-nitrophen and its photolysis photoproducts with Ca^{2+} and includes the competing binding of Ca^{2+} to fura-2. The predicted evolution of $[Ca^{2+}]_i$ to successive flashes matched that observed experimentally when each 200 J flash was assumed to photolyse 30 % of the DM-nitrophen remaining in the cuvette. The model also includes a calculation of the transient rise in $[Ca^{2+}]_i$ that occurs immediately after the rapid photolysis of DM-nitrophen, but before released Ca^{2+} has time to re-equilibrate with the remaining unphotolysed DM-nitrophen. This rebinding occurs on a millisecond time scale (Zucker, 1993).

For calculations of Ca^{2+} transients in cells filled with DM-nitrophen and exposed to light flashes, the same model was used, with the inclusion of competing reactions of unphotolysed DM-nitrophen, its photoproducts, and ATP with Mg^{2+}, and also the binding of Ca^{2+} to a native buffer. Concentrations of 3·5 mM free Mg^{2+}, 3 mM Mg-ATP and 1·25 mM native buffer with an affinity of 12·5 μM were assumed (see Delaney & Zucker, 1990).

Diazo-4. The change in free Ca^{2+} after diazo-4 photolysis was measured by arsenazo spectrophotometry in microcuvettes that had a pathlength similar to the mean cell diameter (i.e. 300 μm). The standard calibration solution (SCS) contained (mM): KCl, 250; NaCl, 50; MgCl, 3; and K-Hepes, 25. The pH was adjusted to 7·5. Test solutions contained the SCS with a mixture of 6 mM diazo-4–0·3 mM arsenazo III and either low (0·2 mM) or high (2·0 mM) total Ca^{2+}. All calibrations were done at 21 °C.

The observed changes in amplitude of the arsenazo signal during a series of flashes were compared with those predicted by a computer model. Details of the model are described in the Appendix. The model accurately predicted the observed Ca^{2+} decrements for successive flashes (at both high and low total Ca^{2+}) assuming that the probability of photolysing each site of diazo-4 was 0·30 at the surface of the cuvette. We consider the model to be reasonably predictive of $[Ca^{2+}]_i$ decrements at the front surface of neurons based on the similarity of results between cuvettes and intact cells seen in a previous study of nitr-5 photolysis (Landò & Zucker, 1989).

Flash artifact. Flashes produced a transient current artifact that obscured the initial 0·5–5 ms of current following the flash. The artifact was observed after the flash in all voltage-clamped cells irrespective of the presence of intracellular photolabile compounds. It showed no apparent dependence on the magnitude of the voltage command or the species of conducted ion. Variability in the size of the artifact precluded the possibility of digital subtraction. This fast, electrical artifact has been noted by other workers in the field using a similar flashlamp (Hadley & Lederer, 1991). The possibility of a longer term increase in leak conductance triggered by the flash was checked by (1) the full return of current to the same level as the control upon return to the holding potential and (2) observing the magnitude of current flow during small hyperpolarizing pulses immediately following the 'flashed' pulse. In approximately one in ten 'flashed' cells the current trace stayed inward relative to the control upon return to the holding potential and leak currents were much larger than control in hyperpolarizing test pulses. Results from damaged cells such as these were discarded.

RESULTS

Effect of unphotolysed diazo-4 on membrane currents

Figure 1*A* shows the results from an experiment in which the effect of increasing concentrations of intracellular diazo-4 on the total current was measured in a NASW–TTX saline. It can be seen that successive injections ultimately eliminated the slowly developing outward current component present at −15 mV and greatly diminished the slow tail current that was normally present after partial repolarization to −25 mV. In three experiments of this type a final cytoplasmic diazo-4 concentration of $2{\cdot}4 \pm 0{\cdot}5$ mM eliminated all of the outward current component, leaving a calcium current that still displayed inactivation. The current that was selectively eliminated by diazo-4 injection was $I_{K(Ca)}$ because the Ca^{2+}-activated non-specific cation component of current ($I_{NS(Ca)}$) is negligible at these potentials (Landò & Zucker, 1989).

Figure 1*B* shows a different experiment in which diazo-4 injection affected the pharmacologically isolated I_{Ca}. In two experiments, progressive injections of diazo-4 to final concentrations of 5·5 and 7·3 mM slowed the decline of I_{Ca} during the first stimulus pulse and diminished the reduction of peak I_{Ca} in a subsequent pulse. In

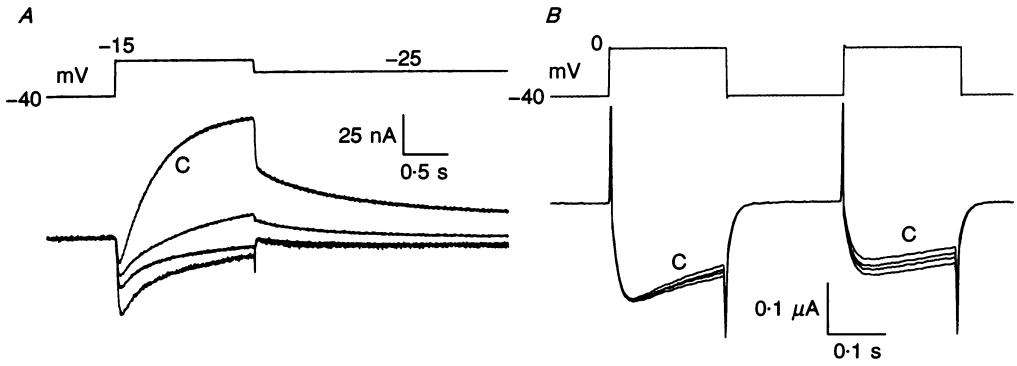

Fig. 1. Effects of succesive intracellular diazo-4 injections on Ca^{2+}-sensitive membrane currents. *A*, total current recorded in zero Na^+, TMA-substituted, 4-AP-containing sea water. Cell L6, 16 °C. No leak subtraction. *B*, pharmacologically isolated I_{Ca} from cell L3, 16 °C. Current in *B* was filtered with a 10 ms time constant. The trace marked C in each panel is the pre-injection control. The lower three traces represent succesive post-injection currents. The total intracellular diazo-4 concentration estimated after the third injection (lowest trace) was 3·0 mM in *A* and 7·3 mM in *B*. CsCl was omitted from the injection solution in these experiments. The outward current blocked by diazo-4 injection in *A* is $I_{K(Ca)}$. The increase in I_{Ca} in *B* represents a true reduction of inactivation since the TEA^+-insensitive component of $I_{K(Ca)}$ is negligible in cell L3 (Deitmer & Eckert, 1985).

all double-pulse experiments the amount of inactivation experienced by the second pulse was determined as 1– (P2/P1) where P1 and P2 are the peak calcium currents attained during the first and second stimulus pulses respectively. Thus in the two experiments mentioned above inactivation was reduced from 0·37 to 0·28 and from 0·42 to 0·25 after diazo-4 injection. The continued presence of I_{Ca} inactivation at diazo-4 concentrations where $I_{K(Ca)}$ was effectively suppressed (≈2 mM) is probably due to the inactivation site being much closer to the calcium channel than the average $I_{K(Ca)}$ channel. For all subsequent I_{Ca} experiments approximately 2 mM intracellular diazo-4 was used, a concentration which helped minimize $I_{K(Ca)}$ contamination while only moderately affecting I_{Ca} inactivation.

Effect of steady diazo-4 photolysis

The aim of preliminary experiments was to confrim that cytoplasmic calcium buffering was increased after diazo-4 photolysis. In these experiments photolysis was achieved using a steady, collimated UV light source. The increase in $[Ca^{2+}]_i$ buffering resulting from such photolysis and its effects on I_{Ca} inactivation are demonstrated in Fig. 2. Figure 2*A* shows the effect of a 1·5 s UV light exposure on the decline of peak I_{Ca} during a train of stimuli at 0·5 Hz. Two effects may be discerned: (1) a reversal of the decline in peak I_{Ca} between pulses 3 and 4 (control

P4/P3 ratio, 0·88; post-UV P4/P3 ratio, 1·9) and (2) a reduction of cumulative inactivation of peak I_{Ca} between pulses 1 and 10 from 0·55 to 0·36.

The smaller peak I_{Ca} in a test pulse (P2) following a conditioning pulse (P1) has been traditionally used as an index of Ca^{2+}-dependent inactivation in *Aplysia*

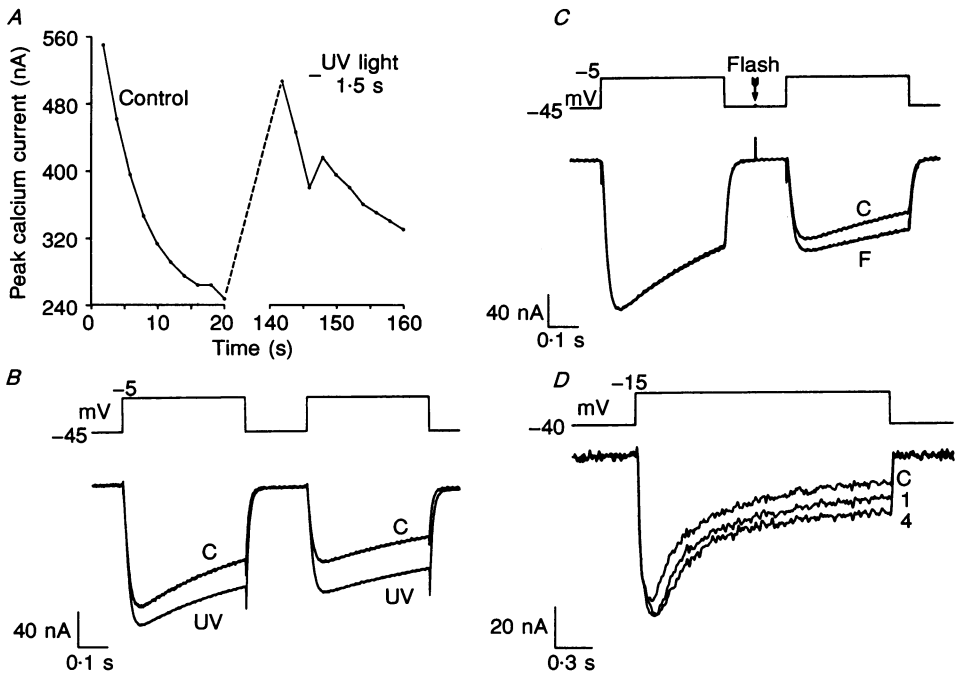

Fig. 2. Diazo-4 photolysis decreases $[Ca^{2+}]_i$-dependent I_{Ca} inactivation. *A*, control Ca^{2+} currents were elicited from a diazo-4-injected L6 neuron by a train of ten 200 ms pulses from −40 to +10 mV at 2 s intervals. A 2 min period was allowed for the recovery of peak I_{Ca} (93 %) after which the train was repeated with a 1·5 s exposure to steady UV light between the third and fourth stimuli (bar). Temperature, 17 °C. *B*, calcium currents in response to two identical depolarizing pulses separated by a 200 ms interval. Two minutes after recording the control traces (C) the cell was exposed to 10 s of steady UV light and the stimulus protocol repeated 30 s later (traces marked UV). Cell L3, 17 °C. *C*, interpulse flash photolysis of diazo-4 rapidly decreases inactivation in the following pulse. A control pair of currents was recorded (C) in response to two identical voltage steps. Two minutes later the protocol was repeated (F) with a 200 J flash given in the middle of the interpulse interval. Cell L6, 17 °C. Current smoothed with a 0·1 kHz Bessel filter. *D*, I_{Ca} inactivation is progressively slowed with successive flashes. Four 200 J flashes were given at 2 min intervals. Trace C is the control, and traces 1 and 4 were recorded 2 min after the first and fourth flashes respectively. Cell L6, 17 °C, 0·03 kHz Bessel filter.

neurons (Tillotson, 1979). Using this protocol, a number of studies (Eckert & Tillotson, 1981; Eckert & Ewald, 1983) have shown that EGTA injection causes (1) an increase in P1 amplitude, (2) a diminished inactivation of peak I_{Ca} in P2 relative to P1, and (3) a decrease in the rate of I_{Ca} relaxation during the depolarizing step. In Fig. 2*B* the effect of prolonged, steady photolysis of diazo-4 on two-pulse I_{Ca} inactivation is shown. After diazo-4 photolysis peak inactivation was reduced from

0·38 to 0·25 and P1 amplitude was increased 14 % indicating a relief of Ca^{2+}-dependent inactivation. The decay time constant (τ) of I_{Ca} in P1 slowed from 270 to 386 ms. There was no significant change in τ for I_{Ca} during P2.

Rapid diazo-4 photolysis between pulses

In subsequent diazo-4 experiments a much faster photolysis was achieved (about 0·4 ms) using a xenon arc flashlamp. This enabled us to see how quickly a sudden drop in $[Ca^{2+}]_i$ could retard the process of inactivation. The result of photolysing diazo-4 in the interval between two pulses is shown in Fig. 2*C*. The dominant effect was an increase in P2 amplitude relative to P1. In three experiments of this kind inactivation was reduced from $0·44 \pm 0·03$ to $0·34 \pm 0·03$.

For relatively long pulses ($\geqslant 1$ s) the I_{Ca} remaining at the end of a depolarizing command is relatively steady and non-inactivating. This component (termed I_∞) has been previously described by Chad, Eckert & Ewald (1984). When a cell injected with diazo-4 was exposed to a series of flashes the most consistent and recognizable effect was a progressive increase in I_∞. Figure 2*D* shows the results from an

TABLE 1. Diazo-4 photolysis at different stages of I_{Ca} decay. Effects on proportional inactivation (PIN) and decay time constant (τ)

Test pulse	Peak I_{Ca} (nA)	I_{Ca} at flash (nA)	PIN (control)	PIN (flash)	$\tau_{control}$ (ms)	τ_{flash} (ms)
−10 mV, 1·5 s	62	19	0·65	0·45	n.d.	n.d.
−15 mV, 1·5 s	52	19	0·37	0·10	n.d.	n.d.
−10 mV, 1·75 s	106	62	0·95	0·68	369	675
−10 mV, 2 s	65	50	0·85	0·72	606	817
−15 mV, 2 s	78	63	0·84	0·68	537	817
−15 mV, 1·5 s	33	29	0·56	0·44	537	681

PIN was determined as $1 - (I_{Ca}$ at the end of the stimulus pulse $/ I_{Ca}$ at the time of the flash) and reflects the proportion of I_{Ca} inactivated with respect to I_{Ca} at the time of the flash. n.d., not determined. All experiments were done at 17 °C.

experiment in which I_{Ca} was recorded 2 min after the first and the fourth 200 J flash (i.e. after full equilibration of photolysed diazo-4 throughout the cell). In four experiments at a test potential of −10 mV, I_∞ (control range 3–9·5 nA) increased from $7·8 \pm 1·9$ % of peak I_{Ca} to $25·5 \pm 5·3$ % after a single 200 J flash, indicating an 18 % reduction in the inactivation from 0·92 to 0·75. In four similar experiments at −15 mV, I_∞ (control range 10–17·5 nA) increased from $17·7 \pm 0·8$ % of peak I_{Ca} to $40·2 \pm 6·1$ %, indicating a 27 % reduction in the inactivation from 0·82 to 0·60. It was noted in two experiments (i.e. Fig. 2*D* and one other experiment where multiple flashes were given) that successive flashes produced diminishing percentage increases in I_∞ and hence decreases in inactivation. Thus the first flash (Fig. 2*D*) decreased inactivation from 0·80 to 0·7 (10 % change) while the next three flashes combined to further decrease it to 0·64 (another 10 % change). There was no change in peak I_{Ca} after a flash in six of ten experiments. In the remaining four, peak I_{Ca} was increased by $12·5 \pm 2·5$ %. No further changes in peak I_{Ca} occurred over the course of another three flashes.

Diazo-4 photolysis during I_{Ca}

Photolysis of diazo-4 during I_{Ca} did not result in any instantaneous increase in I_{Ca} but rather decreased the rate and extent of subsequent inactivation (Fig. 3*A–C*, Table 1). The rate of inactivation was determined by fitting a single exponential to

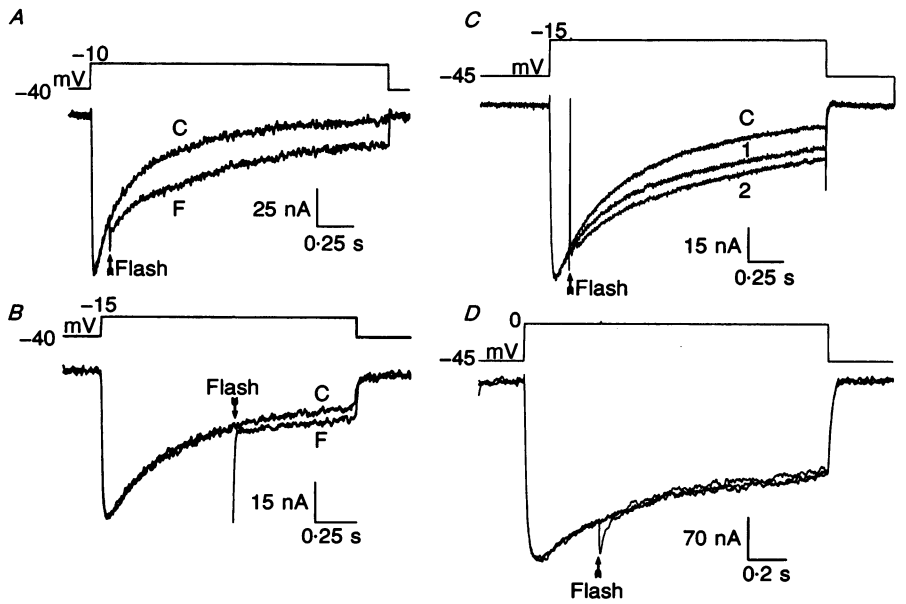

Fig. 3. Flash photolysis of diazo-4 during I_{Ca} rapidly decreases inactivation. *A*, superimposed on the control I_{Ca} (C) is a trace (F) in which a 200 J flash was given 115 ms after the start of the step. The spike-like increase in I_{Ca} immediately following the flash is an electrical artifact (see Methods). Cell L3, 17 °C, 0·1 kHz Bessel filter. *B*, in a different cell, flashing later during I_{Ca} (770 ms after beginning of step) had less effect on inactivation. Cell R15, 17 °C. Same filtering as *A*. *C*, successive flashes progressively decrease I_{Ca} inactivation. C, control trace. In traces 1 and 2 a 200 J flash was given 160 ms after the start of the step. Intersweep interval was 2 min. Peaks have not been normalized. Cell L3, 17 °C. *D*, diazo-4 photolysis has no effect on I_{Ba}. Overlapping traces show I_{Ba} recorded before, during and 2 min after a 200 J flash. The transient inward flash artifact is prolonged by the filtering of the current ($\tau = 5$ ms). No leak subtraction. Cell R15, 17 °C.

the current trace between the point of photolysis and the end of the step. At test potentials of −10 to −15 mV the I_{Ca} was well fitted by a single exponential ($r^2 > 0{\cdot}995$). Table 1 shows that the post-flash decay time constant was increased in each of the four cells where it could be reasonably fitted (i.e. when the flash was given with at least 50 % of the peak I_{Ca} remaining). The mean increase in decay time constant determined from Table 1 was 49·3 ± 12·4 %.

In order to normalize the data from experiments in which the flash was given at different stages of I_{Ca} decay, it was necessary to consider the flash-induced change in current as a proportion of the total amount of inactivation between the point of photolysis and the zero current baseline. In Table 1 the parameter of proportional inactivation (PIN) serves as a normalized indicator of the extent of inactivation after the flash. A control PIN of 0·65 means that 65 % of the current present at the

time of the flash has inactivated by the end of the pulse. In each of the six experiments the PIN decreased after diazo-4 photolysis indicating a decrease in the extent of subsequent inactivation (Table 1). The mean percentage decrease in inactivation induced by a flash (± S.E.M.) was 31·3 ± 8·7 % (range 15·3–73·0 %).

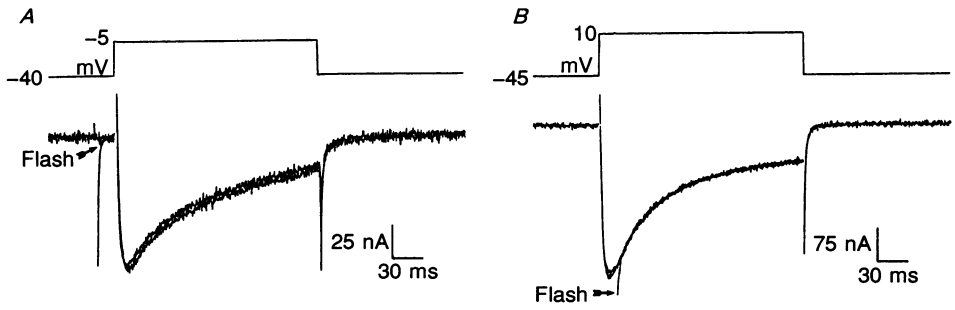

Fig. 4. Ca^{2+} released by nitr-5 photolysis is not sufficient to induce I_{Ca} inactivation. *A* and *B* show typical results from two different neurons previously injected with about 10 mM nitr-5 loaded 70 % with Ca^{2+}. Photolysis before (*A*) or during (*B*) I_{Ca} had no effect on inactivation. Cells L3 and R15. Temperature, 18 °C.

Figure 3*C* illustrates the effect of successive flashes given during I_{Ca}. As was seen in Fig. 2*D*, repeated flashing of the same cell caused incremental (but diminishing) changes in the extent of inactivation. In Fig. 3*C* inactivation at the end of the pulse is reduced from 0·80 to 0·67 by one flash and to 0·62 by the second flash. In one other identical experiment the inactivation changes were from 0·77 to 0·65 to 0·58 respectively.

Diazo-4 photolysis during I_{Ba}

Figure 3*D* shows the superimposition of barium currents recorded before, during and after flash photolysis of diazo-4. The rate of I_{Ba} decay is much slower than that of I_{Ca} and is similar to that of I_{Ca} in EGTA-injected cells (Eckert & Tillotson, 1981). Diazo-4 photolysis had no effect on peak I_{Ba}, the rate of I_{Ba} decay or I_{∞} in four out of four experiments, confirming that relaxation of I_{Ba} is voltage and not Ca^{2+} dependent. The decay from peak I_{Ba} was much less than that of Fig. 3*D* when potentials similar to those used in the I_{Ca} experiments (i.e. −10 to −15 mV) were used.

Inactivation initiated by photolysis of caged calcium

The initiation of Ca^{2+}-dependent inactivation of I_{Ca} was originally attempted with nitr-5 (Fig. 4). Nitr-5 loaded 70 % with Ca^{2+} was pressure injected to a cytoplasmic concentration of about 10 mM. Peak I_{Ca} was decreased by 23 ± 5 % ($n = 15$) after injection. A single 200 J flash was estimated to raise $[Ca^{2+}]_i$ at the inner membrane from 1·4 to 5·2 μM (Landò & Zucker, 1989). Under these conditions, there was no evidence of enhanced inactivation during or after a series of five 200 J flashes (15 experiments).

We next tried the photolabile compound DM-nitrophen, which undergoes a much larger Ca^{2+} affinity change than nitr-5 and thus produces a greater Ca^{2+} jump (Kaplan & Ellis-Davies, 1988; Kaplan, 1990). Photolysis of cytoplasmic DM-nitrophen 10–90 ms before the command step typically reduced peak I_{Ca} by

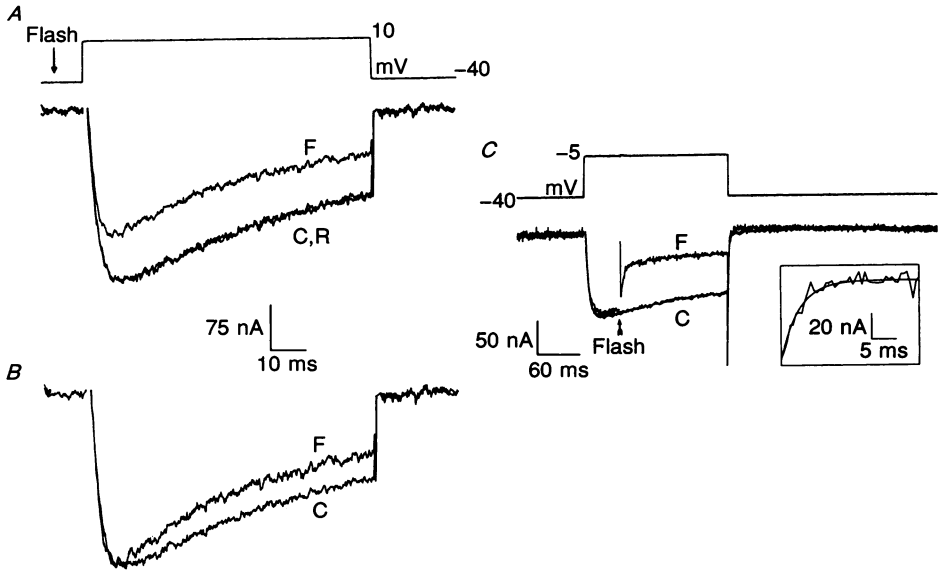

Fig. 5. DM-nitrophen photolysis rapidly blocks I_{Ca}. *A*, I_{Ca} recorded from a neuron injected with 50 % Ca^{2+}-loaded DM-nitrophen to a final intracellular concentration of about 7 mM. Control (C), flash (F) and recovery (R) traces were recorded at 2 min intervals. In trace F a 200 J flash was given at the arrow. *B*, trace F has been normalized to the same amplitude as C (F × 1·366) to demonstrate the acceleration of I_{Ca} decay rate after DM-nitrophen photolysis. Cell L6, 21 °C. *C*, an L3 neuron was injected with 62 % Ca^{2+}-loaded DM-nitrophen and then given a 200 J flash (arrow) during the voltage command. Temperature, 17 °C. C, control; F, flash response. No leak subtraction. Inset: block of I_{Ca} on an expanded time scale showing single-exponential fit (τ = 3·6 ms) after subtraction of I_{Ca} decay during the control step.

30 % (30 ± 3·8 %, n = 4) (Fig. 5*A*). Effects on the decay of I_{Ca} were variable. In two of the experiments (one of which is shown in Fig. 5*B*) the decay time constant (τ) was decreased by 11 and 46 % after the flash despite the reduced amplitude. In the other two experiments, τ was increased 57 and 97 %. Complete recovery from DM-nitrophen-induced inactivation took approximately 2 min (Fig. 5*A*). The intervening recovery period was not studied in detail, but appeared similar to the slow time course of recovery seen in the twin-pulse experiments described later in this paper (see Fig. 8).

DM-nitrophen photolysis during I_{Ca}

The results illustrated in Fig. 5*A* and *B* suggested that the onset of Ca^{2+}-dependent inactivation was rapid. To more accurately discern the kinetics of this

process we photolysed DM-nitrophen during I_{Ca}. Figure 5*C* shows that the Ca^{2+} pulse rapidly inactivated a large portion of I_{Ca} during a step to −5 mV. In five experiments, 41 ± 3 % of I_{Ca} was blocked (relative to the control current at the point of photolysis). The time course of this effect at 17 °C was well fitted (after subtraction of the decay of I_{Ca} during the control step) by a single exponential (Fig. 5*C*, inset) with a time constant of 3·3 ± 0·5 ms ($n = 5$).

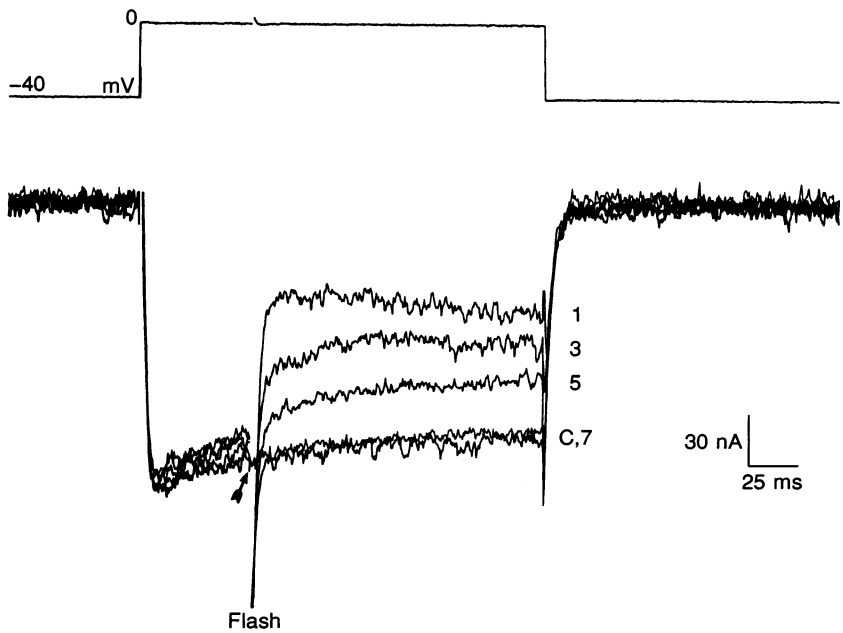

Fig. 6. Rapid block of I_{Ba} by DM-nitrophen photolysis. A sequence of seven 200 J flashes was given at 2 min intervals. The control (C) and the first, third, fifth and seventh flash responses are shown. The small changes in peak I_{Ba} did not vary systematically with successive flashes (lowest to highest peak I_{Ba}: flash 5, 1, 3, C and 7). No leak subtraction. Cell L8, approximately 7 mM DM-nitrophen, 30 % Ca^{2+} loaded, 22 °C.

DM-nitrophen photolysis during I_{Ba}

In two experiments barium currents were recorded in zero Na^+, TEA^+, Ba^{2+} solution, In both cases I_{Ba} was substantially inactivated by photolysis of DM-nitrophen (44 and 35 %). In one of these experiments multiple flash responses were evoked (Fig. 6). Figure 6 shows an overlay of the control I_{Ba} (at 0 mV, 22 °C) and the first, third, fifth and seventh responses in a series of 200 J flashes at 2 min intervals. The block of leak-corrected I_{Ba} (measured at the end of the step as a percentage of the control) for flashes 1, 3, 5 and 7 was 44, 28, 13 and 0 % respectively. For comparative purposes, a single exponential was fitted to the first 25 ms of current after each flash, revealing a progressive slowing of inactivation with successive flashes. Due to noise considerations, reasonable fits ($r^2 > 0·9$) were only determined for the first four flashes. The time constants (flash 1 to flash 4) were 1·7, 2·4, 3·4 and 4·2 ms respectively.

Effects of phosphatase inhibition on inactivation

If inactivation is mediated by Ca^{2+}-dependent activation of phosphatase (Armstrong, 1989) then inhibition of such a phosphatase should decrease inactivaton. We chose the cyclic hepatotoxin microcystin-LR (MLR) in preference to okadaic acid because it is significantly more potent at inhibiting a broad spectrum of phosphatases in *Aplysia* neuronal extracts (Ichinose, Endo, Critz,

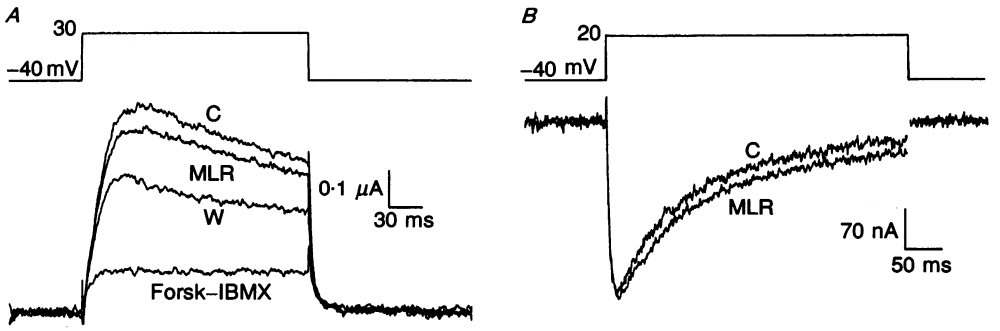

Fig. 7. Microcystin-LR (MLR) reduces $I_{K(V)}$ and sensitizes it to forskolin and IBMX but has little effect on I_{Ca}. *A*, $I_{K(V)}$ was recorded from an R15 neuron before (C) and 30 min after pressure injection of MLR to an intracellular concentration of about 5 μM (MLR). A solution containing forskolin and IBMX was then bath applied and $I_{K(V)}$ recorded 3 min later (Forsk–IBMX) and 20 min after its wash-out (W). Cell R15, 22 °C. *B*, I_{Ca} before (C) and 90 min after (MLR) injection of MLR to 5 μM. No leak subtraction. Cell L3, 18 °C.

Shenolikar & Byrne, 1990; Endo, Shenolikar, Eskin, Zwartjes & Byrne, 1992). Intracellular injection of MLR to concentrations between 0·5 and 5 μM had variable effects on I_{Ca} in five experiments. Forty-five minutes after injection of MLR the following parameters were noted and expressed as a percentage of the control: peak I_{Ca}, 115 ± 26 %; decay time constant, 96 ± 7 %; I_{∞}, 137 ± 36 %. The large standard errors result from one atypical experiment (cell L8) in which MLR increased peak I_{Ca} by 62 % and increased I_{∞} by 49 %. A more typical result is illustrated in Fig. 7*B*. We confirmed that MLR was affecting endogenous protein phosphatases by looking at its effect on $I_{K(V)}$ (Fig. 7*A*). The effect of intracellularly injected MLR (5 μM) alone was a small decrease in peak current (15 ± 5 %, $n = 3$). A more profound effect was a sensitization of the cells to the subsequent addition of forskolin and IBMX (Fig. 7*A*). Thus the normal latency of the forskolin–IBMX effect was dramatically shortened (from 15 to 25 min to < 5 min) and the magnitude of $I_{K(V)}$ block enhanced (from 25 ± 5 to 68 ± 7 %). A cyclic AMP-dependent decrease in $I_{K(V)}$ has previously been reported for *Aplysia* bag cell neurons (Strong & Kaczmarek, 1985).

Effects of cyclic AMP-dependent phosphorylation on recovery from inactivation

The recovery from inactivation measured in twin-pulse experiments characteristically displays bi-exponential kinetics (Tillotson & Horn, 1978; Adams & Gage, 1979; Plant & Standen, 1981) with a fast time constant of tens to hundreds

of milliseconds and a slow time constant of seconds to tens of seconds. In the present experiments we focused on the slow phase of recovery, which should be less influenced by the late opening of Ca^{2+} channels during the long (200 ms) prepulse. Single-exponential fits between interpulse intervals of 0·2 and 20 s typically gave

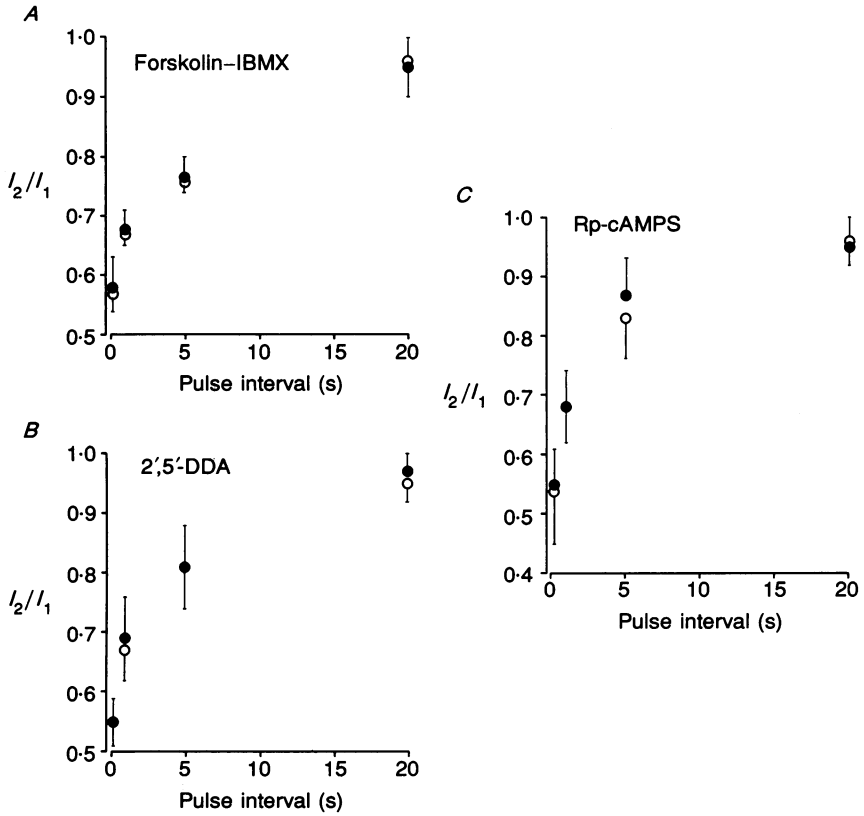

Fig. 8. Slow recovery from inactivation is not dependent on cyclic AMP-dependent phosphorylation. Recovery curves were constructed by measuring peak I_{Ca} during two 200 ms steps from −40 to 0 mV (I_1, I_2) at four different pulse intervals (0·2, 1, 5 and 20 s). ○, control; ●, test solution. *A*, 30 min after bath application of forskolin (100 μM) and IBMX (200 μM). *B*, 25 min after intracellular injection of 1–2 mM DDA. *C*, 30 min after bath application of Rp-cAMPS (200 μM). Where symbols overlap exactly only a filled symbol is shown. All points represent the mean ± 1 S.D. from three experiments. Temperature, 18 °C.

recovery time constants of 1–3 s, with full recovery taking about 30–40 s. If this slow rate of recovery from inactivation reflects the cyclic AMP-dependent rephosphorylation of Ca^{2+} channels then increases in cyclic AMP should speed recovery and decreases should slow recovery.

Increases in cyclic AMP were elicited by bath application of a forskolin–IBMX mixture (F–I) or by a direct pressure injection of cyclic AMP in the presence of IBMX. Figure 8*A* shows results from the three F–I experiments. The recovery curves were virtually identical before and after drug application. Similar results were seen with direct cyclic AMP injection (3 experiments, not shown). Both

methods effectively reduced the peak amplitude of $I_{K(V)}$ (F–I, 25 ± 5 %, $n = 3$; cyclic AMP, 21 ± 3 %, $n = 3$) while having no effect on peak I_{Ca} or subsequent inactivation.

A decrease in cAMP-dependent phosphorylation was effected by (1) inhibition of adenylate cyclase (DDA) or (2) inhibition of cyclic AMP-dependent protein kinase activation (Rp-cAMPS). Intracellular injection of DDA to approximately 1 mM caused a slow decline in peak I_{Ca} that stabilized after 20–30 min at 77 ± 2 % ($n = 3$) of the pre-injection control. There was no significant effect of DDA on I_{Ca} inactivation or its recovery at this time (Fig. 8*B*). Bath application of Rp-cAMPS (200 μM, 30–60 min) had no effect on peak I_{Ca}, inactivation or its recovery (3 experiments, Fig. 8*C*) but fully blocked the usual suppression of $I_{K(V)}$ by forskolin–IBMX application and cyclic AMP injection (4 experiments, not shown).

DISCUSSION

Identification of calcium current studied

Calcium currents in *Aplysia* have recently been shown to be partially separable on pharmacological grounds (Edmonds, Klein, Dale & Kandel, 1990). We have not distinguished different components of I_{Ca}, and can only say our results apply to slowly decaying calcium currents activated by large depolarizations.

Predicting effects of diazo-4 photolysis with a 'shell' model

Injection of 2·5 mM diazo-4 increased peak I_{Ca} slightly and reduced inactivation about 10 % (Fig. 1). Photolysis by a 200 J flash or 2 s of 150 W illumination increased I_{Ca} and reduced inactivation a further 20 % (Fig. 2). Photolysis of diazo-4 during or after a pulse never led to recovery of I_{Ca} or reversal of inactivation (Figs 2 and 3, Table 1), but only reduced inactivation in subsequent pulses by about 30 %.

Photolysis of one diazo-4 molecule produces two H^+ ions (Adams *et al.* 1989). A 200 J flash photolysed about 30 % of diazo-4 at the front surface, so a cell filled with 2·5 mM would release 1·5 mM H^+. Considering the H^+ buffering capacity of *Aplysia* cytoplasm (Zucker, 1981), this should reduce cytoplasmic pH by only 0·025 units, which is unlikely to affect the responses observed.

In our first effort to understand these results, we used a 'shell' model (Smith & Zucker, 1980; Standen & Stanfield, 1982; Chad *et al.* 1984) of the effect of diazo-4 photolysis on submembrane $[Ca^{2+}]_i$ during depolarizations. I_{Ca} was represented as a uniform influx described by a Hodgkin–Huxley-type formula fitted to a typical record. Ca^{2+} diffused inwardly with binding to the various forms of diazo-4 calculated from our model of photolysis (see Appendix) and to 0·44 mM of an immobile buffer of 4.4 μM affinity, similar to that reported in molluscs (Alemà, Calissano, Rusca & Giuditta, 1973; Krinks, Klee, Pant & Gainer, 1988) and identical to singly photolysed diazo-4 to simplify calculations. Ca^{2+} was extruded by uptake into organelles and a surface membrane pump adjusted to match experimental measurements (Smith & Zucker, 1980).

Figure 9 shows predictions of this model. The left column shows $[Ca^{2+}]_i$ in a submembrane shell 0.2 μm thick, and the right column shows $[Ca^{2+}]_i$ at 0·9 μm from the surface. Results with thinner shells were similar. Row *A* is for I_{Ca} like that in Fig. 2*D*; the traces show $[Ca^{2+}]_i$ before and after injecting 2·5 mM diazo, after a

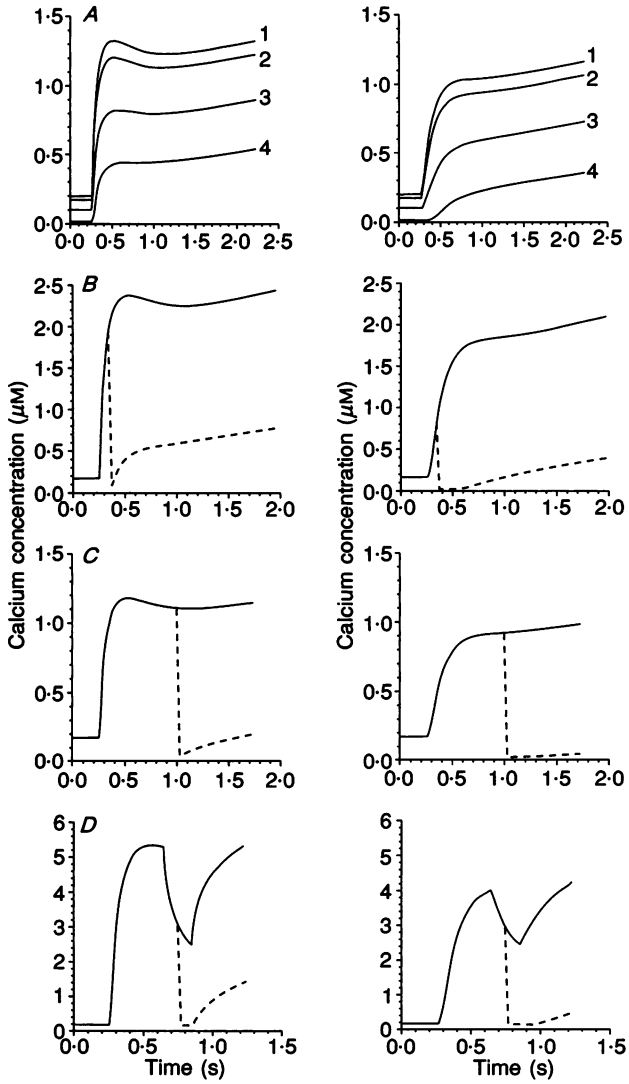

Fig. 9. Calculated effects of diazo-4 photolysis on submembrane $[Ca^{2+}]_i$. Calcium enters the cell at a rate measured in voltage-clamp experiments, diffuses radially inward with binding to a native buffer and to diazo-4, and is actively removed by pumps that reduce the volume-average $[Ca^{2+}]_i$ to 50 % in about 2 s. In each row, the left column represents the outer 0·2 μm thick submembrane shell of cytoplasm, and the right column represents $[Ca^{2+}]_i$ at a distance of 0·8–1·0 μm from the plasma membrane. Row *A*, responses to a Ca^{2+} influx like that of Fig. 2*D*. Trace 1, before injection of diazo-4. Trace 2, after injecting 2·5 mM diazo-4. Trace 3, several seconds after one 200 J flash or 2 s of 150 W illumination to allow diffusional equilibration of the effects of the flash on Ca^{2+}, diazo-4 and its photoproducts. Trace 4, following four flashes, or 8 s of illumination. Rows *B* and *C*, calculated effects of a 200 J flash on $[Ca^{2+}]_i$ in a cell experiencing I_{Ca} similar to those of Fig. 3*A* and *B* respectively. Continuous trace, without flash; dashed trace, flash during depolarizing pulse. Row *D*, calculated effect of a 200 J flash on $[Ca^{2+}]_i$ in a cell with the I_{Ca} of Fig. 2*C*. Continuous trace, currents during two depolarizations without photolysis of diazo-4; dashed trace, flash given between the pulses. In all cases, the calculated effects on $[Ca^{2+}]_i$ are substantially larger than the observed effects on I_{Ca} inactivation.

200 J flash or 2 s of steady 150 W illumination and allowing diffusional equilibration, and after four flashes or 8 s of light. If inactivation is proportional to submembrane $[Ca^{2+}]_i$, the reductions in Ca^{2+} accumulation should resemble the reductions in inactivation of I_{Ca} seen on injecting diazo-4 (Fig. 1), following a 200 J flash (Fig. 2*D*) or 2 s of 150 W light (Fig. 2*A*), and following four 200 J flashes or 10 s of 150 W light (Fig. 2*B* and *D*). The reduction in Ca^{2+} accumulation is about twice the reduction in I_{Ca} inactivation under the various conditions, but otherwise the effects on $[Ca^{2+}]_i$ resemble the effects on inactivation.

Rows *B* and *C* of Fig. 9 show the effects on submembrane $[Ca^{2+}]_i$ and $[Ca^{2+}]_i$ 0·8–1·0 μm from the membrane when a 200 J flash is given during a current similar to that of *A* and *B* respectively of Fig. 3. Submembrane $[Ca^{2+}]_i$ drops below resting level at the flash and accumulates little afterwards. Due to the absorption of UV light by photolabile chelators, the back of the cell remains in the dark, so the immediate effect of a flash on whole-cell I_{Ca} should be half as great as the effect on submembrane $[Ca^{2+}]_i$ at the front surface. In fact, photolysis affected I_{Ca} much less than expected from Fig. 9*B* and *C*. Row *D* of Fig. 9 shows the effect of a 200 J flash presented between two pulses as in Fig. 2*C*. Ca^{2+} accumulation at the front surface is practically abolished during the second pulse, so that whole-cell I_{Ca} inactivation should be reduced to half, while in fact the effect on inactivation during the pulse was much less.

The 'shell' model therefore provides a qualitative, but not quantitative, explanation of the results. Refining the model by increasing I_{Ca} slightly after photolysis has almost no discernible effect on the predictions, and using mobile buffers for diazo-4 photoproducts would only increase the rate of Ca^{2+} diffusion from the membrane and so increase the disagreement with experimental observation.

Implications of the results with nitr-5 and DM-nitrophen

The most serious problem with the 'shell' model is that submembrane $[Ca^{2+}]_i$ never exceeds 1–2·5 μM (depending on the magnitude of I_{Ca} in each experiment). If this level of $[Ca^{2+}]_i$ causes inactivation, then photolysis of nitr-5 should inactivate I_{Ca}. However, even when multiple flashes were used to elevate submembrane $[Ca^{2+}]_i$ to about 5 μM, we saw no effect on I_{Ca}. On the other hand, photolysis of DM-nitrophen, which causes a much larger change in $[Ca^{2+}]_i$, could reduce I_{Ca} (or I_{Ba}) by as much as 50 %, when delivered during (Figs 5*C* and 6) or immediately before (Fig. 5*A*) a depolarizing pulse. Since only the front surface of a 300 μm diameter cell is exposed to significant light intensity (Landò & Zucker, 1989), this result corresponds to a virtual elimination of I_{Ca} at the front surface.

The effects of DM-nitrophen photolysis on I_{Ca} are due to Ca^{2+} rather than H^+ or Mg^{2+} release because (1) the predicted pH change from H^+ release is less than 0·02 units and (2) photolysis of Mg^{2+}-loaded DM-nitrophen failed to affect I_{Ca}. Thirty per cent photolysis of 5 mM DM-nitrophen loaded 50 % with Ca^{2+} should cause front surface $[Ca^{2+}]_i$ to rise from a resting level of 2 μM to about 25 μM at the moment of the flash. Following the flash, $[Ca^{2+}]_i$ would drop after a few milliseconds to 5·3 μM as Ca^{2+} rebinds to unphotolysed DM-nitrophen (Zucker, 1993). The high resting level is caused by competition of Mg^{2+} (3·5 mM free, plus 3·0 mM bound weakly to ATP) with Ca^{2+} for the same binding site on DM-nitrophen.

Since the size of the $[Ca^{2+}]_i$ 'spike' following photolysis is strongly dependent on the intracellular concentration of DM-nitrophen and the level of Ca^{2+} loading, we suggest that our estimates should be taken as approximations. For example, the extent of Ca^{2+} loading could be decreased by the cell's Ca^{2+} extrusion mechanisms. Nevertheless, several important conclusions are possible. (1) DM-nitrophen photolysis inactivated I_{Ca} (or I_{Ba}) within a few milliseconds (Figs 5*C* and 6), so high $[Ca^{2+}]_i$ acts rapidly to close Ca^{2+} channels. (2) A flash preceding a pulse by up to 100 ms inactivated the subsequent I_{Ca} even though $[Ca^{2+}]_i$ would have recovered to the low micromolar range by the time of the stimulus pulse. Since nitr-5 photolysis raises $[Ca^{2+}]_i$ into this range but does not cause inactivation, we suggest that high $[Ca^{2+}]_i$ can inactivate Ca^{2+} channels from their closed state. (3) I_{Ca} recovered fully within 2 min after a flash. Therefore, the reduction in current amplitude is due to the peak rise in $[Ca^{2+}]_i$ right after a flash and not to a residual persistent $[Ca^{2+}]_i$ change. (4) Even though the front surface $[Ca^{2+}]_i$ drops rapidly after DM-nitrophen photolysis, the recovery of I_{Ca} is slow. This is consistent with the diazo-4 result (Fig. 3*A–C*) that shows that a rapid drop in $[Ca^{2+}]_i$ does not rapidly restore I_{Ca}.

Effect of diazo-4 photolysis on calcium near channel mouths

Apparently, only $[Ca^{2+}]_i$ exceeding tens of micromolar causes inactivation. Such levels normally occur only near Ca^{2+} channel mouths. Therefore, a Ca^{2+} channel is likely to be inactivated mainly by the Ca^{2+} that enters through it when it is open. To analyse the effect of diazo-4 photolysis on local $[Ca^{2+}]_i$ near channel mouths, we developed a 'domain' model of Ca^{2+} diffusing spherically away from a channel. A single channel current of 0·35 pA was assumed to last for 1 ms, and this current was doubled to account for diffusion into a semi-infinite space. Ca^{2+} bound to and dissociated from four diffusible buffers at each time step in each 10 nm shell. $[Ca^{2+}]_i$ was calculated out to 1 μm from a channel mouth, where it was negligibly perturbed from rest.

For a native buffer, we assumed an initial concentration of 1 mM, a binding constant of 10^8 M^{-1} s^{-1} and a dissociation rate of 2000 s^{-1}, yielding a dissociation constant of 20 μM. The binding parameters match the quantity and buffering capacity of cytoplasmic buffer measured in molluscan neurons (Smith & Zucker, 1980; Krinks *et al.* 1988); a fast binding rate is assumed by analogy with T-sites of Ca^{2+}-binding protein in muscle (Robertson, Johnson & Potter, 1981), and because transients of unbuffered $[Ca^{2+}]_i$ are not observed to brief Ca^{2+} influx, even on a millisecond time scale (Charlton, Smith & Zucker, 1982). A diffusion constant of 10^{-7} cm^2 s^{-1} was assumed, appropriate for a large protein. The other three buffers were unphotolysed, singly photolysed, and doubly photolysed diazo-4 diffusing at 5×10^{-7} cm^2 s^{-1}. They were assigned a binding rate of 5×10^{-8} M^{-1} s^{-1} (Kao & Tsien, 1988), and the unbinding rates were calulated from the dissociation constants. The starting concentration of each buffer was determined from calculations of the effects of a 200 J flash on diazo-4. Ca^{2+} diffused at a rate of 6×10^{-6} cm^2 s^{-1}.

Table 2 shows the calculated levels of $[Ca^{2+}]_i$ at different distances from a channel mouth at the end of a 1 ms opening. $[Ca^{2+}]_i$ rose to 90 % of these levels within 10 μs, which explains why there is no correlation between the duration of channel opening and the likelihood of subsequent inactivation (Lux & Brown, 1984). The table shows that the effect of injecting, or photolysing, diazo-4 on $[Ca^{2+}]_i$ depends

strongly on distance from the channel mouth. The predicted effects at 20–30 nm match the experimental effects of diazo-4 most closely; that is, they predict about twice the magnitude of effects that we observe for a flash that illuminates only the front half of the cell. They also fit our expectation that DM-nitrophen inactivates channels by elevating $[Ca^{2+}]_i$ to tens of micromolar. We suppose that Ca^{2+} channels inactivate rapidly as they open, and that the development of macroscopic inactivation reflects the progressive inactivation of channels as more and more open. Release of Ca^{2+} from DM-nitrophen inactivates virtually all front surface channels immediately, indicating that closed channels are also inactivated by a rise in $[Ca^{2+}]_i$, but that normally only open channels ever experience a rise in $[Ca^{2+}]_i$ sufficient to inactivate them. If Ca^{2+} acts 20–30 nm from channel mouths, it may act on a separate target protein associated with Ca^{2+} channels. Alternatively, Ca^{2+} may act at a channel site that has obstructed access from the channel mouth, for example, under a rim of the channel.

TABLE 2. $[Ca^{2+}]_i$ near Ca^{2+} channel mouths under different experimental conditions

Experimental condition	$[Ca^{2+}]_i$ (μM) at distance shown from channel mouth				
	5 nm	15 nm	25 nm	35 nm	95 nm
Before injecting chelators	209	73·8	40·5	18·3	5·2
After injecting 2·5 mM diazo-4	199	64·0	33·3	14·7	4·5
At front surface channels immediately after one flash	186	50·9	21·7	6·4	1·1
1 min after one flash, after diffusional equilibration	193	57·8	27·6	10·3	2·3
After injecting 10 mM EGTA	197	62·4	30·4	10·7	1·7
After injecting 10 mM EGTA 95 % loaded with Ca^{2+}	210	74·8	41·5	19·3	6·4

The results so far suggest a channel is inactivated only by Ca^{2+} entering through its own pore. The effect of Ca^{2+} entering through other channels is represented by the 'shell' model (Fig. 9), which predicts too much I_{Ca} inactivation. Moreover, the nitr-5 results show that the expected level of $[Ca^{2+}]_i$ from neighbouring channels is insufficient to initiate inactivation. However, this conclusion is only correct for a uniform distribution of Ca^{2+} channels. If Ca^{2+} channels occur in clusters, then the Ca^{2+} entering through adjacent channels might reach substantially higher concentrations than if channels were evenly distributed as in the 'shell' model, and Ca^{2+} channels might be influenced by ions entering through near neighbours (Mazzanti, DeFelice & Liu, 1991; Imredy & Yue, 1992).

Comparison with other molluscan studies, and effects of buffer injection

Several studies have proposed that $[Ca^{2+}]_i$ inactivates molluscan calcium channels at low micromolar concentrations. Plant *et al.* (1983) and Chad & Eckert (1984) used a 'shell' model to explain inactivation. A non-exponential time course in I_{Ca} decay was attributed to saturation of binding sites at a concentration of a few micromolar. Chad *et al.* (1984) introduced a 'calcium domain' model in which Ca^{2+} acted on the channel through which it entered. They showed that an apparent voltage dependence of inactivation can be explained by a reduction in the single

channel current as the Ca^{2+} equilibrium potential is approached. However, $[Ca^{2+}]_i$ near channel mouths reached only a few micromolar in their coarse-grained diffusion calculations, and this was assumed to saturate the Ca^{2+} binding site in order to generate non-exponential I_{Ca} inactivation with a small fast ($\tau = 70$ ms) component. Finally, Gutnick *et al.* (1989) described voltage- and Ca^{2+}-dependent components of inactivation in snail neurons. Their chief evidence for a voltage-dependent component of inactivation was that the recovery from inactivation was accelerated by a hyperpolarizing pulse. We have confirmed previous observations (Eckert & Tillotson, 1981) that no such voltage-dependent 'repriming' is present in the cells we studied. Gutnick *et al.* (1989) regarded the modest effects of EGTA and BAPTA injection on I_{Ca} as indicating that Ca^{2+} must act at least tens of micrometres away from Ca^{2+} channel mouths, and at concentrations of 1 μM or less. In contrast, our results suggest that Ca^{2+} acts at about 25 nm from channel mouths, at a concentration of about 40 μM, to rapidly inactivate channels that open.

We wanted to know whether a slow buffer like EGTA acting at single channels could have effects similar to those reported. Injection of 10 mM EGTA into snail neurons (Plant *et al.* 1983; Gutnick *et al.* 1989) increased the peak current by about 30 % and reduced the rate and extent of inactivation by a similar amount; injection of 30 mM EGTA in *Aplysia* neurons had similar but larger effects (Chad *et al.* 1984). Assuming association and dissociation EGTA binding constants of $0{\cdot}96 \times 10^7$ M^{-1} s^{-1} and 0·872 s^{-1} (Neher, 1986) and a diffusion constant of 5×10^{-7} cm^2 s^{-1}, we calculate that 10 mM EGTA would reduce $[Ca^{2+}]_i$ 20–30 nm from a channel mouth by about 25 %. Plant *et al.* (1983) and Gutnick *et al.* (1989) also found that EGTA and HEDTA 90–95 % loaded with Ca^{2+}, which elevated resting $[Ca^{2+}]_i$ to up to 10 μM, did not increase peak currents or reduce inactivation, but sometimes reduced the peak current slightly. Table 2 shows that 10 mM EGTA 95 % loaded with Ca^{2+} would allow peak $[Ca^{2+}]_i$ to rise slightly higher near Ca^{2+} channels (and so cause slightly more inactivation), than in the absence of the saturated buffer. The effects of Ca^{2+}–buffer injection may therefore be explained by actions on local $[Ca^{2+}]_i$ near Ca^{2+} channels that open.

A new model of calcium channel inactivation in Aplysia

How can a slowly developing macroscopic inactivation arise from a process of Ca^{2+} acting locally and rapidly to inactivate channels that open? We considered a number of channel kinetic schemes and found that it was necessary to devise a mechanism by which some channels would open quickly, thus leading to an early peak current in about 25 ms, but others would open only after hundreds of milliseconds, to provide a late component of current. In the following scheme,

$$C_1 \underset{k_{21}}{\overset{k_{12}}{\rightleftharpoons}} C_2 \underset{k_{32}}{\overset{k_{23}}{\rightleftharpoons}} O_3 \overset{k_{34}}{\rightarrow} I_4,$$

C_1 and C_2 are closed states, O_3 is the open state, and I_4 is the inactivated state of the channel. The k values are voltage-dependent rate constants except for k_{34}, which is Ca^{2+} dependent, and k_{12} and k_{21}, which do not change. The scheme does not

include recovery from inactivation (see below), which is a very slow process restoring I_4 to C_1 and C_2. In order to fit experimentally observed currents, we had to make two assumptions: (1) k_{12} and k_{21} must be very different, and (2) C_1 and C_2 must be in equilibrium, rather than all channels starting in state C_1.

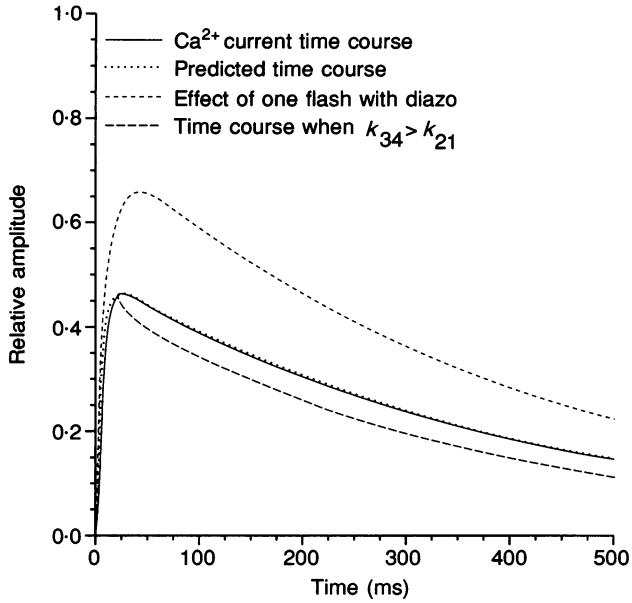

Fig. 10. Dynamic behaviour of the proposed channel kinetic scheme in response to a pulse to 0 mV (dotted line), compared to a typical I_{Ca} time course (continuous line). The short-dashed line is a plot of the calculated effect of photolysis of diazo-4 on I_{Ca} to an immediately following depolarization. The current is enhanced roughly twice as much as is observed in cells in which only half the surface is exposed to the effects of a photolytic flash of light (cf. Fig. 2*D*). The long-dashed line shows that minor adjustments of k_{21} and k_{34} lead to inactivation with a double-exponential time course.

Figure 10 shows the behaviour of this scheme with $k_{12} = 5\ s^{-1}$, $k_{21} = 100\ s^{-1}$, $k_{23} = 0\ s^{-1}$, $k_{32} = 500\ s^{-1}$, and $k_{34} = 100\ s^{-1}$ at rest. On depolarization, k_{32} drops to 0 and k_{23} rises to $100\ s^{-1}$. This establishes a resting equilibrium of 95 % of the channels in state C_1 and 5 % in state C_2, and a rapid deactivation of current at the end of a pulse. On depolarization, channels in state C_2 open rapidly and channels in state C_1 open late. Open channels rapidly inactivate to state I_4. For comparison with the actual behaviour of I_{Ca}, the time course of the predicted macroscopic current is compared to a 'typical' I_{Ca}, using the descriptive equation of activation provided by Chad *et al.* (1984): $I_{Ca} = I_{max}[1 - e^{-t/\tau_m}]^2$, with $\tau_m = 5$ ms, and representing inactivation as the multiplicative factor e^{-t/τ_h}, with $\tau_h = 400$ ms, a value typical of our results. I_{max} was selected to scale the current to the prediction of our kinetic model. Evidently, the time courses are nearly indistinguishable, indicating that such a scheme is capable of replicating the chief characteristics of I_{Ca} kinetics.

The effect of flash photolysis of diazo-4 would be to decrease $[Ca^{2+}]_i$ 25 nm from the open channel mouths by 35 % at the front surface of the cell (Table 2). If we

assume that a single Ca^{2+} ion binds rapidly to a low-affinity site to cause inactivation, then in our kinetic model k_{34} would be reduced proportionately. Reducing k_{34} from 100 to 67 s^{-1} increases peak current 40 % and shifts the peak from 20 to 30 ms, and reduces inactivation slightly. The effects on the peak are about twice those observed (Fig. 2*D*), as expected if only half the cell surface is affected by a flash. The effect on the rate of inactivation is somewhat smaller than seen experimentally.

This scheme also provides a simple explanation for the non-exponential time course of inactivation that is sometimes seen (Chad *et al.* 1984). Either reducing k_{21} or increasing k_{34} so that they are no longer equal achieves this effect. An example, with $k_{21} = 75$ s^{-1} and $k_{34} = 125$ s^{-1} at 0 mV, is shown in Fig. 10.

In conclusion, the simple scheme considered here produces most of the kinetic characteristics of I_{Ca}. We do not claim that the proposed scheme is unique in accounting for inactivation; rather, we have only tried to show that a rapid inactivation of open Ca^{2+} channels by high levels of $[Ca^{2+}]_i$ due to Ca^{2+} entering through that channel can produce the gradual inactivation observed in macroscopic I_{Ca}. In such a scheme, single channels usually open only once, and the probability of being open at a given instant is quite small. In the simulations of Fig. 10, for example, 1·0 on the ordinate corresponds to an open probability of 0·05. These predictions of our kinetic scheme require confirmation from single-channel recordings.

Ca^{2+}-dependent inactivation in other tissues

A number of other studies have suggested that calcium-dependent inactivation is caused by Ca^{2+} acting locally near the channel through which it enters. In chick ventricular myocytes, Mazzanti & DeFelice (1990) found that channels under a patch pipette are not inactivated by Ca^{2+} entering outside the patch. Williams, Pittman & MacVicar (1991) found that Ca^{2+} entering low-threshold channels in rat pituitary melanotrophs failed to inactivate high-threshold channels. In guinea-pig ventricular myocytes, Yue, Backx & Imredy (1990) observed inactivation in patches containing a single Ca^{2+} channel, indicating that L-type Ca^{2+} channels are inactivated by the ions flowing through them. In these channels, inactivation proceeded slowly, and Ca^{2+} appeared to facilitate the return of the channel to a closed state, rather than initiate a rapid transition to an inactivated state. Studying the same cell type, Hadley & Lederer (1991) found that large $[Ca^{2+}]_i$ transients released from photolysis of DM-nitrophen caused inactivation, while smaller $[Ca^{2+}]_i$ steps generated by nitr-5 photolysis increased I_{Ca}, a process not observed in *Aplysia* neurons. In a rat aortic muscle-derived cell line, Giannattasio, Jones & Scarpa (1991) observed that 10 mM BAPTA only partially eliminated Ca^{2+}-dependent inactivation of I_{Ca}. Kay (1991) made a similar observation in guinea-pig hippocampal pyramidal neurons. Kay (1991) also found that 3 μM Ca^{2+} partially blocked inactivation, suggesting an affinity somewhat higher than in *Aplysia*. Finally, Sherman *et al.* (1990) argue that low Ca^{2+} channel densities in mouse pancreatic β-cells require Ca^{2+} to act locally to cause inactivation. They propose that Ca^{2+} binding or a subsequent step is rate limiting, rather than a slow phase of activation as we propose for *Aplysia*.

Molecular mechanism of Ca^{2+}-dependent inactivation

Phosphatases and inactivation

The results provide the first demonstration in intact neurons (Fig. 5*C*) that the onset kinetics of Ca^{2+}-dependent inactivation of I_{Ca} are rapid ($\tau \approx 3$–4 ms at 17 °C). Similar results have been reported for intracellularly perfused neuronal preparations using DM-nitrophen (Morad, Davies, Kaplan & Lux, 1988; Johnson & Byerley, 1991). The rapid block of I_{Ca} suggests direct binding of Ca^{2+} to the inactivation site but does not exclude the possibility of Ca^{2+} channel dephosphorylation by membrane- and Ca^{2+}-dependent phosphatase. We have shown that the phosphatase inhibitor microcystin-LR (MLR) sensitizes $I_{K(V)}$ to the effects of forskolin and IBMX (Fig. 7*A*) but has variable effects on I_{Ca} inactivation. The former effect is presumably due to inhibition of endogenous protein phosphatase (PrP) types 1 and 2A in a manner analogous to the prolongation of the cyclic AMP-mediated suppression of S-K^+ channels previously reported by other laboratories (Ichinose *et al.* 1990). This is consistent with the observation that MLR is 2000 times more potent at inhibiting PrP1 and PrP2A than the Ca^{2+}-dependent PrP2B (calcineurin; Ichinose *et al.* 1990). However, the intracellular concentrations we have used (500–5000 nM) should also have been effective on PrP2B. MLR enhanced peak I_{Ca} and I_{∞} in two of five experiments but had little effect on I_{Ca} in the other three.

This variability of results is reminiscent of the cell-specific variation in the response of I_{Ca} in molluscan neurons to changes in intracellular cyclic AMP (Hockberger & Connor, 1984). The increase in I_{Ca} might thus be related to MLR inhibition of PrP1 and PrP2A rather than calcineurin. Such a mechanism appears to account for the okadaic acid-induced increase in I_{Ca} in cardiac myocytes (Hescheler, Mieskes, Ruegg, Takai & Trautwein, 1988). The unambiguous determination of the participation of calcineurin in I_{Ca} inactivation in *Aplysia* neurons clearly requires the use of a more specific phosphatase inhibitor. In comparative terms it is perhaps relevant that *Aplysia* neurons contain much less calcineurin than mammalian neurons and it appears to be cytosolic in origin rather than membrane bound (Endo *et al.* 1992).

$[Ca^{2+}]_i$, phosporylation and recovery from inactivation

Recovery of I_{Ca} from inactivation induced by nitrophen photolysis or a depolarizing prepulse was slow (Figs 6 and 8), as reported previously (Tillotson & Horn, 1978; Plant & Standen, 1981). The question arises as to whether recovery is Ca^{2+} dependent or Ca^{2+} independent. Evidence for the former comes from two-pulse experiments in which the rate of recovery of peak I_{Ca} in the test pulse was accelerated by the intracellular application of EGTA or BAPTA (Eckert & Tillotson, 1981; Eckert & Ewald, 1983; Yatani, Wilson & Brown, 1983; Gutnick *et al.* 1989). However, increased I_{Ca} in the test pulse might be due to less inactivation occurring as channels open in the presence of EGTA rather than representing a true re-opening of channels previously inactivated during the prepulse. This idea is supported by the results of Fig. 3 where it is clear that a sudden drop in $[Ca^{2+}]_i$ does not increase I_{Ca} (i.e. does not re-open previously inactivated channels) but rather

slows the further onset of inactivation. This result stands in sharp contrast to the rapid step-like decrease in $I_{K(Ca)}$ seen when diazo-4 is photolysed during a pulse (M. W. Fryer & R. S. Zucker, unpublished observations). Thus, the time course of $I_{K(Ca)}$ is directly influenced by the level of $[Ca^{2+}]_i$ at the membrane surface while the rate of recovery of I_{Ca} from inactivation is limited by a much slower process. It is possible that recovery from inactivation is limited by a very slow dissociation of bound Ca^{2+} from the inactivation site.

The most likely Ca^{2+}-independent enzymatic mechanism responsible for slow recovery has been considered to be rephosphorylation by a cyclic AMP-dependent protein kinase (Eckert & Chad, 1984; Chad & Eckert, 1986; Chad, 1988; Armstrong, 1989). If this mechanism controls recovery of I_{Ca} in intact neurons then changes in endogenous kinase activity should change the rate of recovery. We found that neither inactivation nor its recovery rate was affected by increases and decreases in adenylate cyclase activity (Fig. 8*A* and *B*) or direct prevention of cyclic AMP-dependent protein kinase activation (Fig. 8*C*). These treatments have been shown to be effective on K^+ currents in this preparation and K^+ and Ca^{2+} currents in other preparations (Grega & Macdonald, 1987; Hescheler & Trautwein, 1988; Wang, Salter & McDonald, 1991). Chad (1988) also found that recovery from inactivation was independent of the kinase concentration in dialysed *Helix* neurons. These results strongly suggest that recovery from inactivation is not due to calcium channel rephosphorylation by a cyclic AMP-dependent protein kinase. Whether a different kinase system is involved in recovery remains to be tested.

APPENDIX

Computational model of diazo-4 photolysis

In order to interpret the effects of photolysis of diazo-4 on I_{Ca}, we needed to know how this buffer would be affected by flashes of light when injected into cells. For this purpose, a computer model was devised that was similar in structure to one described earlier (Landò & Zucker, 1989). Briefly, the model begins by calculating $[Ca^{2+}]_i$ from the simultaneous solution of equilibrium binding equations for unphotolysed diazo-4 and 0·5 mM of a native cytoplasmic Ca^{2+} buffer with an affinity of 5 μM that holds resting $[Ca^{2+}]_i$ at 200 nM. Next, a flash converts a portion of diazo-4 at the front surface to its photoproducts, and the front surface $[Ca^{2+}]_i$ is recalculated by simultaneous solution of the binding equations for diazo-4, its photoproducts, and the native buffer. This predicts the effect of a flash on the $[Ca^{2+}]_i$ at the front surface of the cell, and provides the new mixture of Ca^{2+} buffers present there shortly after a flash. The volume-average light intensity is calculated from the absorbance of cytoplasm and diazo-4 to the photolytically effective wavelength of light (360 nm), and this is used to predict the volume-average conversion of diazo-4 to its photoproducts and the $[Ca^{2+}]_i$ in the cell after diffusional equilibration takes place. Since $[Ca^{2+}]_i$ never reached high levels in diazo-4 experiments, no provision for Ca^{2+} extrusion or uptake was included. The volume-average mixture of diazo-4 and its photoproducts can be used as a starting point for calculation of the effects of additional flashes on the front surface of the cell, or on the bulk cytoplasm after diffusional equilibration, which takes about 2 min in 300 μm diameter cells (Landò & Zucker, 1989).

Diazo-4 was chosen rather than diazo-2 because the fully photolysed product shows a large enhancement in Ca^{2+}-binding affinity. The photolysis is complicated by the fact that one molecule of diazo-4 can absorb one photon and undergo a 40-fold increase in affinity, or two photons to increase affinity 1600 times. Furthermore, in 10 % of the effective photon absorptions, the active diazoacetyl site is converted to an inactive form with similar affinity to unphotolysed diazo-4, but which is not subject to further photolysis. Thus, after partial photolysis, diazo-4 exists as six species – fully photolysed, one site unphotolysed and one site inactivated, and doubly inactivated (all with low affinity), singly photolysed, and singly photolysed and singly inactivated (both with medium affinity), and doubly photolysed (with high affinity). The conversion probabilities were calculated for each of nine possible transitions (fully photolysed to any of the five remaining forms, singly photolysed to doubly photolysed or to singly photolysed and singly inactivated, and singly inactivated to doubly photolysed or to singly photolysed and singly inactivated), as a function of light intensity. For example, suppose a flash affected each active site with probability P, with P_1 probability (0·9 P) of photolysing the site and probability P_2 (0·1 P) of inactivating the site. Then the transition probability for converting unphotolysed diazo-4 to the singly inactivated form is $2P_2(1 - P_1 - P_2)$. Thus the effect of a flash of a given intensity on the concentrations of the different species of diazo-4 could be computed. To calculate the effects on $[Ca^{2+}]_i$, Ca^{2+} dissociation constants of 180 μM, 4·4 μM, and 110 nM were used for unphotolysed, singly photolysed, and fully photolysed diazo-4, corrected from the values in 100 mM KCl (Adams *et al.* 1989) for the ionic strength of marine cytoplasm and assuming an ionic strength dependence similar to that of nitr-5 (Tsien & Zucker, 1986).

Diazo-4 was generously supplied by Drs S. R. Adams and R. Y. Tsien. Russell English provided valuable technical assistance. We thank Gary Yellen for providing an efficient algorithm for generating equations in the time domain of the behaviour of channel kinetic shemes by inversion of the state transition matrix to find the eigenfuctions. This work was supported by NIH grant NS15114 to R.S.Z. and NH and MRC (Australia) C. J. Martin Fellowship to M.W.F.

REFERENCES

ADAMS, D. J. & GAGE, P. W. (1979). Characteristics of sodium and calcium conductances produced by membrane depolarization in an *Aplysia* neurone. *Journal of Physiology* **289**, 143–161.

ADAMS, S. R., KAO, J. P. Y., MINTA, A., GRYNKIEWICZ, G. & TSIEN, R. Y. (1988). Biologically useful chelators that release Ca^{2+} upon illumination. *Journal of the American Chemical Society* **110**, 3212–3220.

ADAMS, S. R., KAO, J. P. Y. & TSIEN, R. Y. (1989). Biologically useful chelators that take up Ca^{2+} upon illumination. *Journal of the American Chemical Society* **111**, 7957–7968.

ALEMÀ, S., CALISSANO, P., RUSCA, G. & GIUDITTA, A. (1973). Identification of a calcium-binding, brain specific protein in the axoplasm of squid giant axons. *Journal of Neurochemistry* **20**, 681–689.

ARMSTRONG, D. & ECKERT, R. (1987). Voltage-activated calcium channels that must be phosphorylated to respond to membrane depolarization. *Proceedings of the National Academy of Sciences of the USA* **84**, 2518–2522.

ARMSTRONG, D. L. (1989). Calcium channel regulation by calcineurin, a Ca^{2+}-activated phosphatase in mammalian brain. *Trends in Neurosciences* **12**, 117–122.

CHAD, J. (1989). Inactivation of calcium channels. *Comparative Biochemistry and Physiology* A**93**, 95–105.

CHAD, J., ECKERT, R. & EWALD, D. (1984). Kinetics of calcium-dependent inactivation of calcium current in voltage clamped neurons of *Aplysia californica*. *Journal of Physiology* **347**, 279–300.

CHAD, J. E. (1988). Control of the generation and removal of calcium-mediated inactivation of the calcium current in *Helix aspersa* neurons. In *Calcium and Ion Channel Modulation: A Tribute to Roger Eckert*, ed. GRINNEL, A. D., ARMSTRONG, D. & JACKSON, M. B., pp. 197–214. Plenum Press, New York.

CHAD, J. E. & ECKERT, R. (1984). Calcium domains associated with individual channels can account for anomalous voltage relations of Ca-dependent responses. *Biophysical Journal* **45**, 993–999.

CHAD, J. E. & ECKERT, R. (1986). An enzymatic mechanism for calcium current inactivation in dialysed *Helix* neurones. *Journal of Physiology* **378**, 31–51.

CHARLTON, M. P., SMITH, S. J. & ZUCKER, R. S. (1982). Role of presynaptic calcium ions and channels in synaptic facilitation and depression at the squid giant synapse. *Journal of Physiology* **323**, 173–193.

DEITMER, J. W. & ECKERT, R. (1985). Two components of Ca-dependent potassium current in identified neurones of *Aplysia californica*. *Pflügers Archiv* **403**, 353–359.

DELANEY, K. R. & ZUCKER, R. S. (1990). Calcium released by photolysis of DM-nitrophen stimulates transmitter release at squid giant synapse. *Journal of Physiology* **426**, 473–498.

ECKERT, R. & CHAD, J. E. (1984). Inactivation of Ca channels. *Progress in Biophysics and Molecular Biology* **44**, 215–267.

ECKERT, R. & EWALD, D. (1983). Inactivation of calcium conductance characterized by tail current measurements in neurons of *Aplysia californica*. *Journal of Physiology* **345**, 549–565.

ECKERT, R. & TILLOTSON, D. (1981). Calcium-mediated inactivation of the calcium conductance in caesium-loaded giant neurones of *Aplysia californica*. *Journal of Physiology* **314**, 265–280.

EDMONDS, B., KLEIN, M., DALE, N. & KANDEL, E. R. (1990). Contributions of two types of calcium channels to synaptic transmission and plasticity. *Science* **250**, 1142–1147.

ENDO, S., SHENOLIKAR, S., ESKIN, A., ZWARTJES, R. E. & BYRNE, J. H. (1992). Characterization of neuronal protein phosphatases in *Aplysia californica*. *Journal of Neurochemistry* **58**, 975–982.

FRYER, M. W. & ZUCKER, R. S. (1990). Photolysis of the caged Ca^{2+} chelator Diazo-4 rapidly decreases Ca^{2+} accumulation and Ca^{2+} channel inactivation in *Aplysia* neurones. *Society for Neuroscience Abstracts* **16**, 1171.

FRYER, M. W. & ZUCKER, R. S. (1991). Kinetic differences between the onset and recovery of Ca^{2+}-dependent calcium channel inactivation. *Society for Neuroscience Abstracts* **17**, 958.

GIANNATTASIO, B., JONES, S. W. & SCARPA, A. (1991). Calcium currents in the A7r5 smooth muscle-derived cell line. Calcium-dependent and voltage-dependent inactivation. *Journal of General Physiology* **98**, 987–1003.

GREGA, D. S. & MACDONALD, R. L. (1987). Activators of adenylate cyclase and cyclic AMP prolong calcium-dependent action potentials of mouse sensory neurons in culture by reducing a voltage-dependent potassium conductance. *Journal of Neuroscience* **7**, 700–707.

GUTNICK, M. J., LUX, H. D., SWANDULLA, D. & ZUCKER, H. (1989). Voltage-dependent and caldium-dependent inactivation of calcium channel current in identified snail neurones. *Journal of Physiology* **412**, 197–220.

HADLEY, R. W. & LEDERER, W. J. (1991). Ca^{2+} and voltage inactivate Ca^{2+} channels in guinea-pig ventricular myocytes through independent mechanisms. *Journal of Physiology* **444**, 257–268.

HESCHELER, J., MIESKES, G., RUEGG, J. C., TAKAI, A. & TRAUTWEIN, W. (1988). Effects of a protein phosphatase inhibitor, okadaic acid, on membrane currents of isolated guinea-pig cardiac myocytes. *Pflügers Archiv* **412**, 248–252.

HESCHELER, J. & TRAUTWEIN, W. (1988). Modification of L-type calcium current by intracellularly applied trypsin in guinea-pig ventricular myocytes. *Journal of Physiology* **404**, 259–274.

HOCKBERGER, P. & CONNOR, J. A. (1984). Alteration of calcium conductances and outward current by cyclic adenosine monophosphate (cAMP) in neurons of *Limas maximus*. *Cellular and Molecular Neurobiology* **4**, 197–207.

ICHINOSE, M., ENDO, S., CRITZ, S. D., SHENOLIKAR, S. & BYRNE, J. H. (1990). Microcystin-LR, a potent protein phosphatase inhibitor, prolongs the serotonin- and cAMP-induced currents in sensory neurons of *Aplysia californica*. *Brain Research* **533**, 137–140.

IMREDY, J. P. & YUE, D. T. (1992). Submicroscopic Ca^{2+} diffusion mediates inhibitory coupling between individual Ca channels. *Neuron* **9**, 197–207.

JOHNSON, B. D. & BYERLY, L. (1991). Control of neuronal calcium currect by intracellular calcium *Biomedical Research* **12**, suppl. 2, 49–52.

KAO, J. P. Y. & TSIEN, R. Y. (1988). Ca^{2+} binding kinetics of fura-2 and azo-1 from temperature-jump relaxation measurements. *Biophysical Journal* **53**, 635–639.

KAPLAN, J. H. (1990). Photochemical manipulation of divalent cation levels. *Annual Review of Physiology* **52**, 897–914.

KAPLAN, J. H. & ELLIS-DAVIES, G. C. R. (1988). Photolabile chelators for the rapid release of divalent cations. *Proceedings of the National Academy of Sciences of the USA* **85**, 6571–6575.

KAY, A. (1991). Inactivation kinetics of calcium current of acutely dissociated CA1 pyramidal cells of the mature guinea-pig hippocampus. *Journal of Physiology* **437**, 27–48.

KRAMER, R. H. & ZUCKER, R. S. (1985). Calcium-dependent inward current in *Aplysia* bursting pace-maker neurones. *Journal of Physiology* **362**, 107–130.

KRINKS, M. H., KLEE, C. B., PANT, H. C. & GAINER, H. (1988). Identification and quantification of calcium-binding proteins in squid axoplasm. *Journal of Neuroscience* **8**, 2172–2182.

LANDÒ, L. & ZUCKER, R. S. (1989). 'Caged calcium' in *Aplysia* pacemaker neurons. Characterization of calcium-activated potassium and nonspecific cation currents. *Journal of General Physiology* **93**, 1017–1060.

LUX, H. D. & BROWN, A. M. (1984). Single channel studies on inactivation of calcium currents. *Science* **225**, 432–434.

MAZZANTI, M. & DEFELICE, L. J. (1990). Ca channel gating during cardiac action potentials. *Biophysical Journal* **58**, 1059–1065.

MAZZANTI, M., DEFELICE, L. J. & LIU, Y.-M. (1991). Gating of L-type Ca^{2+} channels in embryonic chick ventricle cells: dependence on voltage, current and channel density. *Journal of Physiology* **443**, 307–334.

MORAD, M., DAVIES, N. W., KAPLAN, J. H. & LUX, H. D. (1988). Inactivation and block of calcium channels by photoreleased Ca^{2+} in dorsal root ganglion neurons. *Science* **241**, 842–844.

NEHER, E. (1986). Concentration profiles of intracellular calcium in the presence of a diffusible chelator. *Experimental Brain Research* **14**, 80–96.

PLANT, T. D. & STANDEN, N. B. (1981). Calcium current inactivation in identified neurones of *Helix aspersa*. *Journal of Physiology* **321**, 273–285.

PLANT, T. D., STANDEN, N. B. & WARD, T. A. (1983). The effects of injection of calcium ions and calcium chelators on calcium channel inactivation in *Helix* neurones. *Journal of Physiology* **334**, 189–212.

ROBERTSON, S. P., JOHNSON, J. D. & POTTER, J. D. (1981). The time-course of Ca^{2+} exchange with calmodulin, troponin, parvalbumin, and myosin in response to transient increases in Ca^{2+}. *Biophysical Journal* **34**, 559–569.

SHERMAN, A., KEIZER, J. & RINZEL, J. (1990). Domain model for Ca^{2+}-inactivation of Ca^{2+} channels at low channel density. *Biophysical Journal* **58**, 985–995.

SIMON, S. M. & LLINÁS, R. (1985). Compartmentalization of the submembrane calcium activity during calcium influx and its significance in transmitter release. *Biophysical Journal* **48**, 485–498.

SMITH, S. J. & ZUCKER, R. S. (1980). Aequorin response facilitation and intracellular calcium accumulation in molluscan neurones. *Journal of Physiology* **300**, 167–196.

STANDEN, N. B. & STANFIELD, P. R. (1982). A binding-site model for calcium channel inactivation that depends on calcium entry. *Proceedings of the Royal Society* B **217**, 101–110.

STRONG, J. A. & KACZMAREK, L. K. (1985). Multiple components of delayed potassium current in peptidergic neurons of *Aplysia*: Modulation by an activator of adenyl cyclase. *Journal of Neuroscience* **6**, 819–822.

TILLOTSON, D. (1979). Inactivation of Ca conductance dependent on entry of Ca ions in molluscan neurons. *Proceedings of the National Academy of Sciences of the USA* **77**, 1497–1500.

TILLOTSON, D. & HORN, R. (1978). Inactivation without facilitation of calcium conductance in caesium-loaded neurones of *Aplysia*. *Nature* **273**, 312–314.

TSIEN, R. & ZUCKER, R. S. (1986). Control of cytoplasmic calcium with photolabile 2-nitrobenzhydrol tetracarboxylate chelators. *Biophysical Journal* **50**, 843–853.

WANG, L., SALTER, M. W. & MCDONALD, J. F. (1991). Regulation of kainate receptors by cAMP-dependent protein kinase and phosphatases. *Science* **253**, 1132–1135.

WILLIAMS, P. J., PITTMAN, Q. J. & MACVICAR, B. A. (1991). Ca^{2+}- and voltage-dependent inactivation of Ca^{2+} currents in rat intermediate pituitary. *Brain Research* **564**, 12–18.

YATANI, A., WILSON, D. L. & BROWN, A. M. (1983). Recovery of Ca currents from inactivation : the roles of Ca influx, membrane potential and cellular metabolism. *Cellular and Molecular Neurobiology* **3**, 381–395.

YUE, D. T., BACKX, P. H. & IMREDY, J. P. (1990). Calcium-sensitive inactivation in the gating of single calcium channels. *Science* **250**, 1735–1738.

ZUCKER, R. S. (1981). Tetraethylammonium contains an impurity which alkalizes cytoplasm and reduces calcium buffering in neurons. *Brain Research* **208**, 473–478.

ZUCKER, R. S. (1992). Effects of photolabile calcium chelators on fluorescent calcium indicators. *Cell Calcium* **13**, 29–40.

ZUCKER, R. S. (1993). The calcium concentration clamp: spikes and reversible pulses using the photolabile chelator DM-nitrophen. *Cell Calcium* **14**, 87–100.

ZUCKER, R. S. & FOGELSON, A. L. (1986). Relationship between transmitter release and presynaptic calcium influx when calcium enters through discrete channels. *Proceedings of the National Academy of Sciences of the USA* **83**, 3032–3036.